FEM Analysis Applied to Electric Machines for Electric Vehicles

JUAN DE SANTIAGO OCHOA

Dissertation presented at Uppsala University to be publicly examined in Polhemsalen, Ångströmlaboratoriet, Lägerhyddsvägen 1,, Uppsala. Friday, October 7, 2011 at 13:15 for the degree of Doctor of Philosophy. The examination will be conducted in English.

Abstract
de Santiago Ochoa, J. 2011. FEM Analysis Applied to Electric Machines for Electric Vehicles. Acta Universitatis Uppsaliensis. *Digital Comprehensive Summaries of Uppsala Dissertations from the Faculty of Science and Technology* 845. 54 pp. Uppsala. ISBN 978-91-554-8136-0.

Electric vehicle technology is an interdisciplinary field in continuous development. It appears to be a margin for improvements. The Division for Electricity at Uppsala University is doing significant research in the field. The present thesis investigates electric machines for vehicular applications, both in the driveline and in the traction motor.

Section 1 presents a driveline with two galvanically isolated voltage levels. A low power side is operated at the optimum voltage of the batteries, while a high power side is operated at a higher voltage leading to higher efficiencies in the traction motor. Both sides are coupled through a flywheel that stabilizes the power transients inherent to a drive cycle.

A review of electric machine topologies for electric vehicles is presented in Section 2. The permanent magnet excited machine is the most suitable technology for an electric driveline.

Section 3 is devoted to numerical models applied to electric machines. The equivalent circuit of a motor/generator with two sets of windings is first presented. This machine couples both sides of the driveline and drives the rotor of the flywheel. The electric parameters are calculated with custom FEM models. A discussion on slotless machines concludes with a simple model to analyze the magnetic field from one static 3D simulation. The tooth ripple losses in solid salient poles are also analyzed with a novel FEM approach. A complete description of the losses in electric machines gives a proper background for further discussion on efficiency.

Section 4 presents the experimental work constructed to validate the theoretical models. The experiments include an axial flux, single wounded prototype, an axial flux, double wound prototype and a planed radial flux coreless prototype.

Section 5 focuses on traction motors for electric vehicles. A simulated prototype illustrates a design and calculation process. The loss theory and the numerical methods presented in Section 3 are applied.

Juan de Santiago Ochoa, Uppsala University, Department of Engineering Sciences, Electricity, Box 534, SE-751 21 Uppsala, Sweden.

List of Papers

This thesis is based on the following papers, which are referred to in the text by their Roman numerals.

I   **Santiago, J.**, Oliveira, J. G., Lundin, J., Abrahamsson, J., Larsson A., and Bernhoff H. (2009) Design Parameters Calculation of a Novel Driveline for Electric Vehicles. *World Electric Vehicle Journal*. Vol. 3.

II   **Santiago, J.**, and Bernhoff H. (2010) Comparison between axial and radial flux PM coreless machines for flywheel energy storage. *Journal of Electrical Systems*. Vol. 6, Issue 2.

III   **Santiago, J.**, Larsson A., and Bernhoff H. (2010) Dual Voltage Driveline for Vehicle Applications. *International Journal of Emerging Electric Power Systems*. Vol. 11, Issue 3.

IV   Oliveira, J. G., Lundin, J., **Santiago, J.**, and Bernhoff H. (2010) A Double Wound Flywheel System under Standard Drive Cycles: Simulations and Experiments. *International Journal of Emerging Electric Power Systems*. Vol. 11, Issue 4.

V   **Santiago, J.**, and Bernhoff H. (2011) 3D FEM modeling of ironless Axial Flux Permanent Magnet motor/generators. *Journal of Electrical and Electronics Engineering*. Vol. 4, Number 1, Pp. 53-58.

VI   **Santiago, J.**, Oliveira, J. G., Lundin, J., Larsson A., and Bernhoff H. (2008) Losses in Axial-Flux Permanent-Magnet Coreless Flywheel Energy Storage Systems. *Proceedings of the 18th International Conference on Electrical Machines ICEM*, Vilamoura, Portugal, September 6-9, 2008.

VII   **Santiago, J.**, Oliveira, J. and Bernhoff, H., Filter Influence in Rotor Losses in Coreless Axial Flux Permanent Magnet Machines, Submitted to *Journal of Electrical Systems*.

VIII   **Santiago, J.**, Bernhoff, H., Ekergård, B., Eriksson, S., Ferhatovic, S., Waters, R., and Leijon, M., "Electrical Motor Drivelines in Commercial All Electric Vehicles: a Review", Submitted to *IEEE Transactions on Vehicular Technology*.

IX   **Santiago, J.**, and Bernhoff, H., "Tooth Ripple Losses in Solid Salient Pole Synchronous Machines with Concentrated Windings," Submitted to *IEEE Transactions on Energy Conversion*.

The author has contributed to other publications which are not incorporated in this thesis, these are as follows:

X **Santiago, J.**, and Oliveira, J. (2010) Electric machine topologies in energy storage systems. *Energy Storage, Chapter 1.* Sciyo, ISBN 978-953-307-119-0.

XI Abrahamsson, J., **Santiago, J.**, Oliveira, J. G., Lundin, J., and Bernhoff H. (2010) Prototype of electric driveline with magnetically levitated double wound motor. *International Conference on Electrical machines ICEM.* Rome, 2010.

XII **Santiago, J.**, Oliveira, J. G., Lundin, J., Abrahamsson, J., Larsson A., and Bernhoff H. (2009) Design Parameters Calculation of a Novel Driveline for Electric Vehicles. *International Battery, Hybrid and fuel cell electric vehicle symposium and exhibition, EVS- 24th.* Stavanger, Norway, 13-16 May 2009.

XIII Larsson A., Bernhoff H., Hogdin, S., **Santiago, J.**, Bolund, B., and Nyholm, S. E. (2007) Construction, modeling and evaluation of a low-loss motor/generator for flywheel energy storage. *7th International All-Electric Combat Vehicle Conference*, Stockholm, Sweden, 11-13 June 2007.

XIV M. Leijon, B. Ekergård, S. Eriksson, S. Ferhatovic, **J. de Santiago**, H. Bernhoff and R. Waters, "On a Two pole motor for Electric Propulsion System," Submitted to *IEEE Transactions on Vehicular Technology*.

Contents

Abbreviations

Acronyms

AC	Alternating Current
AFDW	Axial Flux Double Wounded
AFPM	Axial Flux Permanent Magnet
AFSW	Axial Flux Single Wounded
BDFM	Brushless Doubly Feed Machine
DC	Direct Current
EV	Electric Vehicle
FEM	Finite Element Methods
HEV	Hybrid Electric Vehicle
IC	Internal Combustion
IM	Induction Motors
PES	Primary Energy Source
PM	Permanent Magnet
RM	Reluctance Motors
SB	Synchronous Brushed
SoC	State of Charge
TPL	Two Power Level
TVLM	Two Voltage Level Machine
UPS	Uninterruptible Power Supply

Symbols

Symbol	Unit	Definition
A	m^2	Area
B	T	Magnetic flux density
B_r	T	Remanent magnetic flux density
C_f	-	Drag friction coefficient
E	V	Back emf.
E	V	Electric field
E_r	J	Rotational energy
J	$kg \cdot m^2$	Moment of inertia

J	A/m^2	Current density
H	A/m	Magnetic field
I	A	Current
L	Ohm	Inductance
M	Ohm	Mutual inductance
P	W	Power
Q	J/kg	Energy density
R	Ohm	Resistance
T	^oK	Temperature
X_{sd}	Ohm	Reactance in direct axis
X_{sq}	Ohm	Reactance in quadrature axis
b	m	Radius of strands in a conductor
e	-	Emissivity
emf	V	Electromagnetic force
h	$W/(m^2 \cdot {}^oK)$	Heat transfer coefficient
i	A	Phase current
k	$W/(m \cdot {}^oK)$,	Material's thermal conductivity,
$k_{bearing}$	$W/(rad/s)$	Bearing friction coefficient
k_{drag}	$W/(rad/s)^3$	Drag friction coefficient
k_e	$W/(T\ rad/s)^{1.5}$	Excess losses coefficient
k_h	$W/(T^{ks}\ rad/s)$	Hysteresis losses coefficient
k_s	-	Steinmetz coefficient
l	m	Length
r	m	Radius
δ	m	Skin depth
δ	rad	Power angle
$λ_M$	Wb	Flux linkage
ξ	rad	Angel between set of windings
ρ	kg/m^3	Density
ρ	Ohm·m	Resistivity
σ	$W/(m^2 \cdot {}^oK^4)$	Stefan–Boltzmann constant
σ	Pa	Tensile strength
ω	rad/s	Rotational speed
$μ_0$	V·s/(A·m)	Permeability of free space
$μ_r$	-	Relative magnetic permeability
$θ_R$	rad	Angle of the rotor positions
$Φ_R$	Wb	Rotor magnetic flux

1. Introduction

There is nothing more practical than a good theory

Kurt Lewin

1.1 Background

The work presented in this licentiate thesis is part of the Electric Energy Storage project developed at the Division for Electricity at Uppsala University. The group at the Division of Electricity is doing research in the improvement of electric vehicles, and more specifically in the development of a new electric driveline with two isolated voltage levels and flywheel energy storage.

The research topics of the group include electric motor/generators, power electronics, magnetic bearings and system simulations of the two voltage level driveline. This thesis focuses on the motor/generator design and calculation although results from other fields are presented as the motor/generator is studied from the system perspective.

1.2 All electric vehicles status and forecast

The electric propulsion history starts as early as at the first half of the nineteen century. Electric Vehicles (EVs) dominated the market until the break through of the Ford T model. The aim for lower fuel consumption led to the first Hybrid Electric Vehicle (HEV), the Lohner-Porsche developed in 1899. Engineers realized that higher efficiencies could be achieved if internal combustion (IC) motors operate in combination with electric traction motors.

Environmental concerns and oil prices have drawn attention to HEVs and EVs again. The main advantage of electric propulsion is the pipe emission free capability, while all possible drawbacks appear to be technically solvable. All but one: the price. All prognoses agree that electric drivelines will never be price competitive, even considering economies of scale, with traditional gasoline motors. This statement is reflected in dada of Fig. 1.1 for HEVs, while EVs should show similar disheartening figures. The cost analysis of different components presented in Fig. 1.2 shows the bottleneck of the popularization of EVs [1].
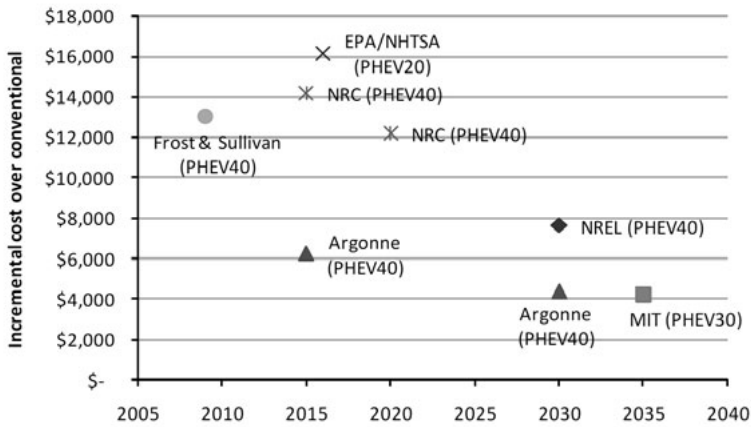
Figure 1.1. Estimation of plug-in hybrid vehicles' incremental manufacturing cost over conventional vehicles. Figure reprinted from [1].
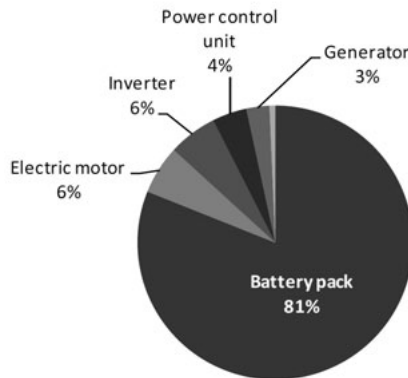

Figure 1.2. Breakdown of PHEV drive system cost by component. Figure reprinted from [1].

There are many arguments for the EVs other than retail prices. We should pay attention to the price rather than the costs. The environmental situation of modern cities makes the use of IC engines unsustainable. Air pollution causes the premature death of 370,000 people each year within the EU [2], 394,000 in China [3] and increasing worldwide. There is a social and political determination to increase the air quality for health but also for economic reasons. European Commission intends to eliminate conventionally-fuelled cars in cities by 2050 [4]. In the near future the EV will most likely be not only a mayor player in private transportation; the EV will be the only player.

A look at the breakdown of the EV's driveline costs may direct the research to the battery where more economic gain is possible. However improvements in the electric motor and power electronics may be more cost effective. Small gains in efficiency reduce the demand on the batteries. An increase of 8% in the efficiency of the electric motor would reduce the bat-

tery demands enough to pay back the whole cost of the electric motor. This scenario is realistic as today's electric cars use inefficient induction motor with as low efficiency as 75% [5].

1.3 Kinetic Energy Storages – Flywheels

Any rotating device stores energy in form of kinetic energy due to the attribute moment of inertia. A flywheel is a part of a rotational system that is design intentionally to have a high moment of inertia. This simple concept has been use since ancient times in the potter's wheel and it is mounted in every combustion engine at the end of the crank shaft to smooth their operation. Modern flywheel energy storage systems consist of an integrated electric motor/generator and a power conversion system.

The improvement of advanced materials and power electronics has dramatically increase the fields of application which now include aerospace [6], Uninterruptible Power Supply (UPS) [7], grid quality enhancement [8], integration of renewable sources in the grid [9] and vehicles [10]. There are nowadays commercial flywheels where this technology is taking the place of other storing technologies such as batteries. Some properties that make flywheels optimal for certain applications are:

- High power density.
- High energy density.
- No capacity degradation. Lifetime is independent of the deep of discharge.
- The state of charge is easily and accurately measurable since it is given by the rotational speed.
- Long life and little maintenance.
- Environmentally friendly. Built with harmless materials.

The kinetic energy stored in a flywheel is proportional to the moment of inertia J and to the square of its rotational speed ω according to (1.1).

$$E_r = \frac{1}{2} J \cdot \omega^2 \qquad (1.1)$$

Due to the proportionality to the square of the rotational speed, a decrease in 50% in the speed corresponds to a 75% energy discharge. So a variation in speed represents a more than proportional variation in the state of charge. An increase in the operational speed involves a substantial increase in the energy stored. The strategy to increase the energy should be focus on increasing the rotational speed. Moreover, the moment of inertia is proportional to the weight, so an increase on the moment of inertia produces an increase on the energy, but not on the energy density.

The materials and designs employed for flywheels have changed since the first stone, concrete and steel applications. High strength composite materials such glass fibers and carbon fibers are applied in high speed flywheels. These materials have much higher ultimate strength limit σ in circumferential than in radial direction. To make the most of this anisotropic property, rims are preferred over disc designs, where the stress in more evenly distributed. The hub is made of a light material such aluminum alloys. The maximum energy density in a thin rim, considering neither the hub nor the motor/generator becomes:

$$Q = \frac{\sigma}{2 \cdot \rho} \tag{1.2}$$

Table 1.1 presents the maximum energy density Q and density ρ for different suitable materials for rotors [11]. The energy density presented in Table 1.1 is calculated for a constant stress shape disc and is twice the values given by equation (1.2).

Table 1.1 Tensile strength and maximum potential energy density data for different rotor materials. Data presented in reference [11].

Material	Density (kg/m^3)	Tensile strength (MPa)	Max energy density	Cost ($/kg)
4340 Steel	7700	1520	0.19 MJ/kg = 0.05 kWh/kg	1
E-glass	2000	100	0.05 MJ/kg = 0.014 kWh/kg	11
S2-glass	1920	1470	0.76 MJ/kg = 0.21 kWh/kg	24.6
Carbon T1000	1520	1950	1.28 MJ/kg = 0.35 kWh/kg	101.8
Carbon AS4C	1510	1650	1.1 MJ/kg = 0.30 kWh/kg	31.3

The speed of the flywheel is only limited by the tensile strength and can be expressed with the maximum peripheral speed. Thus the rotational speed may be increased with smaller radius. Higher rotational speeds lead to higher energy density but reduce the efficiency of the electric motor/generator over certain speed. Nominal power in electric machines is usually limited by thermal constrains. There is a recommended maximum nominal power for electric machines [12]:

$$P(kW) \leq \frac{6.2 \cdot 10^6}{(rpm \cdot 1{,}000)^{3.3}} \tag{1.3}$$

Eq. (1.3) is plotted with examples of high speed machine, some of them with power rates over recommendations. Eq. (1.3) is a recommendation and not a physical law, but it discourages extreme high speed ratings. Parallel

flywheels are a commonly used option when higher power rates are required. The relation between power and speed is addressed in Paper II.
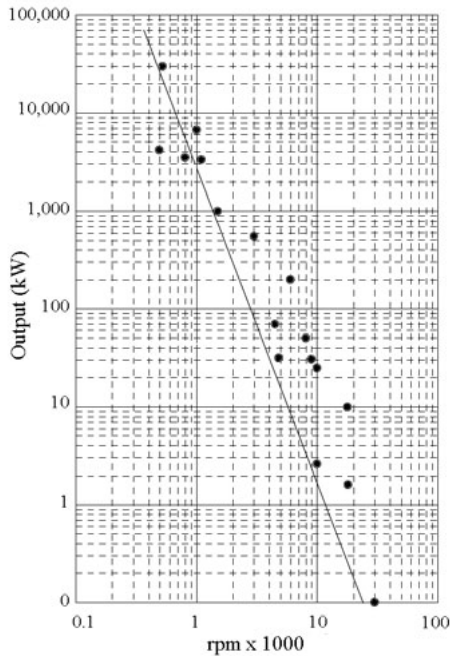

Figure 1.3. Power and speed of examples of high speed motors and the output power limit recommendation from eq. 1.3. Figure reprinted from [12]

1.4 Flywheel Applications

The description of modern flywheel concepts based on a composite rotor and driven by an electric machine started in the 1970s and 1980s [13]. It is therefore a relatively new field of research based on the latest developments in strong light weight composites, new magnetic materials, magnetic bearings and power electronics. Despite the short history of the field, there are already commercial applications and other uses have been identified:

- Space applications

Some navigation systems in airplanes and satellites are based on gyroscopes. NASA has been developing an integrated power and altitude control base on a high speed flywheel [6]. High speed flywheels are potentially smaller and lighter than the NiH_2 battery systems employed today [14].

- UPS

UPS systems are employed when a reliable power supply is needed such as in healthcare, data centers and other industrial applications where power fluctuations may be dangerous for people or cause severe economical losses. Traditional UPS consist of battery packs with less initial investment but higher losses, maintenance, not environmentally friendly chemicals. Main UPS manufacturers include flywheel units in their portfolio [15 17].

Flywheels for UPS differ slightly from on board applications as they are stationary and are not limited by size or weight. The flywheels are not operated at as high speeds but are made in high strength composite materials. The efficiency is claimed to be up to 98% [15].

- Grid quality enhancement and renewable integration.

The electric system requires instantaneous balance of demand and generation of power. The electric system may be enhanced with a flywheel energy storage system that absorbs energy when it is in abundance, and then discharge energy during peaks in the demand [18] and [19]. This grid regulation is traditionally made with water pumped storage power stations [20], but there are a limited number of locations with favorable orography. The flywheel storage system may be also frequency sensitive and respond to frequency variations.

The power grid enhancement is especially important in small or weak power systems, pulsating loads like arc furnaces, unbalance loads like in railways substations and to increase the penetration of variable energy sources. Renewable energy sources such as wind required a back up energy as the power is predictable only in near future. Power systems with high renewable energy sources penetration usually has gas or diesel power plants running idle as reserve. Flywheel systems can play this roll with positive environmental and economic impact.

- Vehicles

There have been several attempts to use flywheels as energy storage systems in vehicles. The first commercial application reported goes back to 1950's in an electric bus called Gyrobus [21]. The energy storage system was base on a three-ton steel flywheel attached to an electric motor/generator. The flywheel was recharged at bus stops, where the motor would accelerate the flywheel up to around 3.000 rpm. Once charged, a Gyrobus could travel around 6 km. The development of modern power electronics improved the performance of flywheels as energy storage source. There are currently several research groups investigating applications in busses [22], trams [10] and heavy vehicles [24] and [25].

Flywheels in vehicles are used as a primary energy source [10], as a component of the drive train in hybrid vehicles [26] and as a subsystem in the DC power bus in the driveline of electric vehicles [27]. The TVLM investi-

gated in this thesis is part of a novel drive line intended to increase the efficiency and life time of batteries in electric vehicles.

1.5 Two Voltage Level Driveline

The driveline proposed in the Electric Energy Storage working group in the Division for Electricity is presented in Fig. 1.4. Batteries are the Primary Energy Source (PES) but the same concept is also applicable to fuel cells. The novelty is that batteries and traction motors operate at their optimum level, instead of using a compromise battery voltage level for a common DC bus.
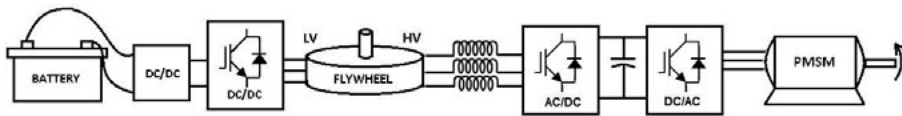

Figure 1.4. Two Power Level driveline configuration for All Electric Vehicles.

The traction motor is connected to the High Power side capable to handle power transients. The battery is connected to the Low Power side and delivers power smoothly. Both voltage sides are coupled through an electric synchronous machine with two sets of windings placed in its stator. This motor/generator, referred as Two Voltage Level Machine (TVLM), transfers power back and forth from both sides and stabilizes the power transients absorbing and releasing energy from a flywheel.

This new driveline concept with Tow Power Levels (TPL) is illustrated in Fig 1.4. The High Power side of the TVLM is linked bi-directionally to the traction motor that operates at higher voltage than the batteries and delivers power to the wheels. When the vehicle brakes, the energy is recovered and stored in the flywheel. For long regenerative braking times the energy flow is reversed from the flywheel to recharge the battery.

Traditional electric vehicle drivelines, even with flywheels, are based on a single DC power bus link [28]. The benefits of having two voltage rates and power levels in the driveline are that the wheel motors operate at higher voltages with higher efficiencies, independently of the optimum voltage of the PES. The presence of a flywheel guarantees a smooth energy flow from the PES, reducing the power stress and increasing the efficiency and lifetime of the components. The system additionally adds freedom in the choice of PES. There is a trade off between the power density, energy density and life time of batteries. With the addition of the flywheel, low power battery packs with large specific energy and long life may be used, prolonging the range of the vehicle.

2. Electric machines for variable speed operation

> What has been will be again,
> what has been done will be done again;
> there is nothing new under the sun.
> <div align="right">Ecclesiastes</div>

2.1 Electric machine topologies

There is a great variety of electric machine topologies, almost one for each application. The following description focuses on traction motors for electric vehicles presented in Paper VIII; the description is extended to electric machines for energy storage applications in Paper X.

DC

The stator of a DC motors consists of a stationary magnetic field. It is generally induced by stator coils but it is also produce by permanent magnets in low power rated machines. The magnetic field in the rotor is also induced by a DC current switched by a commutator. The commutator is a mechanical device at the end of the rotor. The rotating part is a segmented steel surface connected to the rotor coils. The coils are in contact with stationary coal brushes electrified with a DC voltage. When the rotor turns the commutator ensures that the contact between the brushes and the rotor coils gives the maximum torque in the rotor. A representation of a DC motor is illustrated in Fig. 2.1.
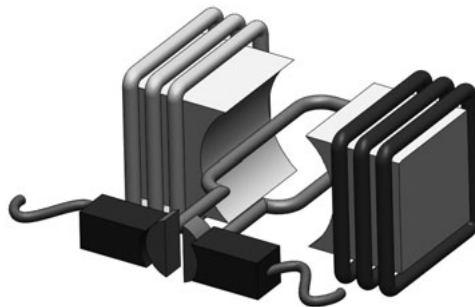

Figure 2.1. Schematic representation of a DC motor.

This type of motor is still widely use in small and medium size vehicles because the technology is well established, they are inexpensive and the control is simple and robust. DC motors were the preferred option in variable

speed applications before the development of advanced power electronics. Presently the technology has become obsolete due to the maintenance needs, dust from the brushes and the poor efficiency compared to other electric machines [29].

Induction

Induction Motors (IM) are very robust due to their rotor construction. The rotor consists of a stack of laminated steel reinforced with short-circuited aluminum bars in the shape of a squirrel cage. The magnetic field induced in the stator is trapped though the rotor bars. When the stator magnetic field rotates at a slightly different speed than the rotor the currents induced in the rotor bars creates a torque. The torque characteristics of the machine are determined by the shape of the rotor bars. A representation of the rotor is presented in Fig. 2.2.
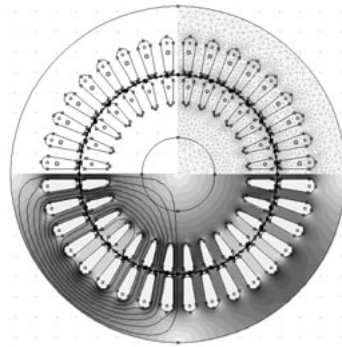

Figure 2.2. Representation of a four pole Induction motor in a FEM package. The sketch, mesh and solution with the magnetic flux and the vector potential lines are shown in the four quadrants.

Presently induction motors are the most used in vehicular propulsion. The efficiency and power density is higher than DC motors although efficiencies as low as 75% are reported in [5].

Reluctance

Reluctance Motors (RM) have salient poles like in stepper motors. The torque is produced solely by the difference between the direct axis and quadrature axis synchronous reactance as the rotor lacks excitation. The stator can have distributed windings like IMs or concentrated windings. The schematic representation of a RM with concentrated windings is presented in Fig. 2.3.
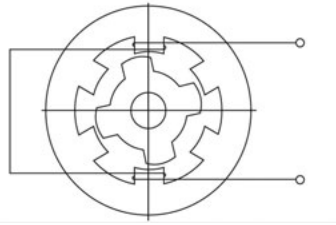
Figure 2.3. Reluctance motor with concentrated windings representation.

RMs are not as widespread as IMs due to their more complex control, but they have analog characteristics in terms of efficiency and power density. A breakthrough is expected as the power electronic technology evolves and RMs present better performance than Induction machines for several applications. For example ABB has announced recently that they now offer RM that fulfills the IE4 super premium efficiency regulation [30].

Synchronous brushed

Synchronous Brushed (SB) motors have been selected by Renault for their electric vehicle portfolio [31]. In this configuration the rotor is wound and excited with a direct current from brushes through slip rings, not through a commutator. Fig. 2.4. shows a schematic representation.
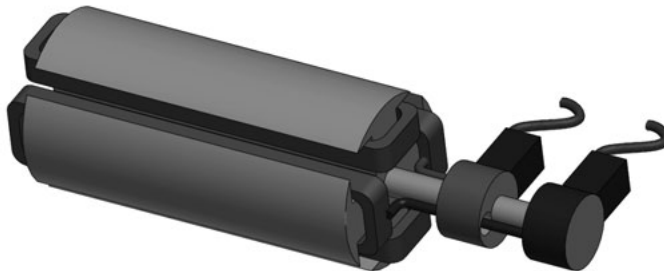

Figure 2.4. Synchronous brushed motor representation.

The peak efficiency is lower than other type of motors because of the Joule losses in the rotor. However, the regulation of the magnetic excitation is simple and accurate, which dramatically reduces the losses at partial loads. SB motors present very good performance for partial loads [32], has high starting torque, it is very robust, has a simple control and the slip rings are maintenance free compared to commutators.

Permanent Magnet

The development of high energy density and high coercivity magnetic materials has increased the design possibilities of Permanent Magnet (PM) mo-

tors and generators. PM machines are self excited, i. e. that the rotor creates its own magnetic field without excitation currents which generate losses. New neodymium magnets ensure high magnetic flux density in the air gap combining high power density and high efficiency.

PM machines allow great design flexibility. Axial flux configurations are also popular for in wheel motors, beside traditional radial flux geometry.

Halbach arrangement is a special magnet configuration, both for axial and radial flux machines. In an ideal Halbach array, the magnets are combined in such a way that the magnetic flux density is cancelled in one side of the array. With a Halbach array no magnetic back-iron is needed and higher specific torques may be achieved [33]. This concept is clarified in Fig. 2.5.
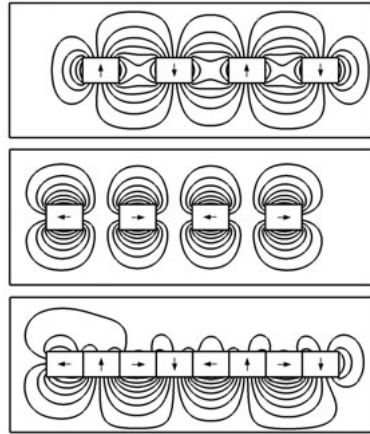

Figure 2.3. Halbach array construction scheme.

The magnets are mounted in the rotor in different ways. Axial flux machines usually have their magnets mounted on the surface of the rotor, while radial flux machines may have the magnets either surface mounted or internal mounted. Internal mounted magnet machine properties varies with the geometry and configuration of the rotor. A soft magnetic material conducts the magnetic flux so the magnets are isolated from the harmonics produced by the stator. The iron bridges may be mechanized to obtain a better magnetic flux distribution and to produce significant saliency [34]. The difference between surface mounted and internal mounted magnets is presented in Fig. 2.6.
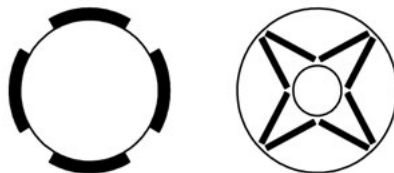

Figure 2.6. Rotors with surface mounted and Internal mounted magnets.

The saliency affects the performance of electric motors as it leads to higher synchronous reactance in the direct axis (X_{sd}) than in the quadrature axis (X_{sq}). For a three phase salient pole synchronous motor with negligible stator winding resistance, the electromagnetic power is expressed as

$$P = 3 \cdot \left[\frac{V \cdot E}{X_{sd}} \cdot \sin(\delta) + \frac{V^2}{2} \cdot \left(\frac{1}{X_{sq}} - \frac{1}{X_{sd}} \right) \cdot \sin(2 \cdot \delta) \right] \qquad (2.1)$$

where V is the input phase voltage, E is the emf induced by the rotor excitation flux and δ is the power angle, for further reading [35].

Stator windings are placed in laminated steel slots since Jonas Wenström invented the slotted armature in 1880. The stator teeth reduce the air gap and therefore the magnetic reluctance in the magnetic circuit. Lower magnetic reluctance leads to lower magnetization currents or less magnetic material, more compact designs and higher power density. But smaller air gaps have also some disadvantages, like higher iron losses in the teeth at high speed. There are two other stator configurations without teeth. In slotless machines the windings are directly placed over the stator yoke. In the ironless or coreless configuration, the back iron yoke rotates simultaneously with the rotor, so the magnetic circuit does not produce hysteresis or eddy current losses. Coreless machines are used in high speed applications with high performance demands [36] and [37]. An ironless radial flux machine with an outer rotor configuration is presented in Fig. 2.7.
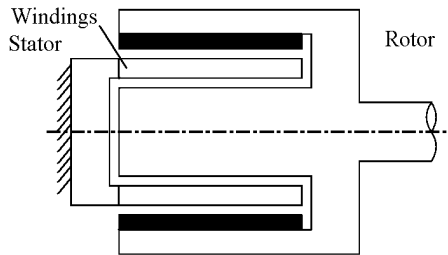

Figure 2.7. Ironless Radial flux machine with an outer rotor configuration.

PM machines also have drawbacks; the magnetization can not be controlled, the permanent magnets are fragile and the operational temperature is limited due to demagnetization. The price of raw materials is also an issue.

2.2 Multiple phase and doubly feed systems

Multiphase power systems have profound advantages over one phase systems. The phase currents sum zero in the case of balanced systems requiring

no returning conductor. The angular shift between phases generates rotating magnetic fields useful to energize AC motors.

Three is the lower number of phases required to have a multiphase balance system and has been adopted as a standard worldwide. There are, nevertheless, examples of systems that use more than three phases. The exceptions are as old as the standard [38]. Systems with more than three phases are use to achieve lower current rate per phase, which the breakers and disconnecting switches carry, more uniform magnetic flux in rotating machines and less voltage ripple at the rectifier output. Using two three-phase parallel systems is a way to take advantage of high phase numbers and within the three phase standard. This concept has been around since 1920's [39]. The two independent sets of windings are placed in the stator with an optimal phase sift of 30º [40]. The combination of two sets of windings is also useful from the control point of view. The Brushless Doubly-Feed Machine (BDFM), used in wind power generation, is the most usual type of double feed machines. One set of windings is directly coupled to the grid while the other is connected to power control unit. The great advantage of this kind of double feed machines is that the power rate of the power electronics is only about 25% of the power [41].

There are also examples of uncommon machines with two sets of windings in the stator with independent use. The Powerformer, for example, has two sets of windings in the stator rated at different voltage levels. The main windings deliver power to the grid at high voltage. The second set of windings is rated at lower voltage levels to supply the ancillary services. [42].

Before the development of power electronics, inverters where DC motors coupled to AC generators. An interesting variant of this system is presented for railroads [43]. A brushless DC motor has an extra set windings in the stator. The shaft drives the air conditioner system and induces voltage in the secondary windings used as a three-phase power source. The kinetic energy stored in the rotor is also claimed to be enough to supply power under short periods of time under loose of contact with the pantograph [44].

Optimal Energy Systems has created a aircraft launch system with a flywheel energy storage module with two sets of windings. The flywheel receives the power at low voltage and delivers the energy stored in 2.8 seconds pulses through the secondary set of windings rated up to 1,750 V [45]. The motor/generator chosen in this application is an axial flux coreless machine.

3. Calculation of two voltage level machines

> With four parameters I can fit an elephant, and
> with five I can make him wiggle his trunk.
>
> John von Neumann

3.1 Equivalent circuit

Electric machines, and in particular PM motors and generators, are described by well established equations and equivalent circuit representations [35]. A balanced three phase machine is studied through a one phase equivalent circuit defined by resistances, inductances, capacitances and voltage sources. The basic equivalent circuit of a permanent magnet synchronous machine is shown in Fig. 3.1.
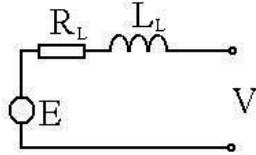

Figure 3.1: One-phase equivalent circuit of a permanent magnet synchronous motor/generator.

L_L stands for the line inductance, obtained by adding the shelf and mutual inductances between phases. V represents the line voltage, E the back electromotive force and R_L the line resistance. The equation that governs the equivalent electric circuit presented in Fig. 3.1 is:

$$V = R_L \cdot I + \frac{d}{dt} L_L \cdot I + E \tag{3.1}$$

The back emf is calculated through:

$$E = -\frac{d}{dt} \lambda_M = -\frac{d}{dt} N \cdot \Phi_R \cdot \theta_R \tag{3.2}$$

The Two Voltage Level Machine (TVLM) under consideration has two sets of three phase windings with magnetic coupling between them in the stator [46]. The TVLM can operate as a motor and a generator between two power buses at different power rates. The turn ratio determines the back emf of the voltage sides as deduced from equation (3.2). Fig. 3.2 shows the equivalent circuit of the TVLM. The rotor is magnetically linked to both sets of stator windings, but the stator windings are also magnetically linked to each other like in a transformer with a mutual inductance. However, distinct

from a transformer, the voltages in the windings sets are not determined by the transformation ratio straight forward but by the mutual magnetic coupling together with the electromotive force induced by the rotor.
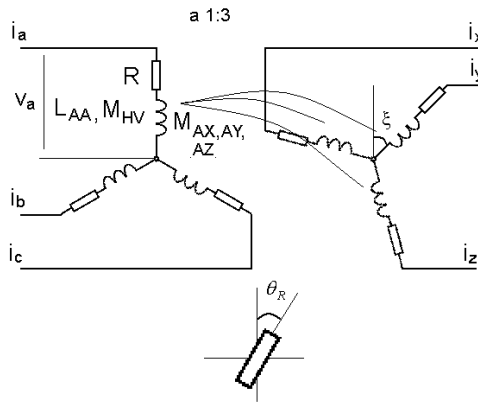

Figure 3.2: Schematic of a Two-Voltages Level Machine (TVLM).

The angle ξ is the shift angle between winding sets, while θ_R represents the rotation of the magnetic field. Therefore, the voltage induced in both high power and low power sets of windings are also shifted an angle ξ.

A TVLM has two windings in the stator with magnetic coupling. The power flows from the low to the high power side in a similar way as in a transformer due to the mutual inductance. However, the output power is not determined by the input power as in transformers. The difference between the input and output energy is the energy stored or delivered by the flywheel.

The one-phase equivalent circuit is shown in Fig. 3.3. The sub index L refers to the Low Power winding set and H refers to the High Power side, or the set of windings with higher number of turns per pole and phase and therefore higher induced emf. L_{HL} is the mutual inductance between both sets of windings. A voltage source connected to the Low Power side (V_L) representing the motor drive, and an inductive load making the High Power side (L and R) acting as a generator. The TVLM can be evaluated as two synchronous machines with a magnetic coupling and common rotor speed. When the load at the High Power side is replaced by a voltage sources, the equivalent circuit represents regenerative breaking from the traction motor.
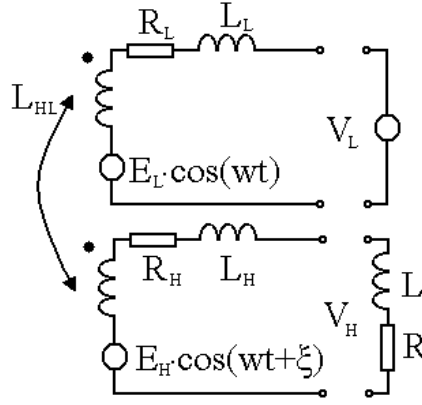
23

Figure 3.3 Equivalent circuit of a TVLM. The high voltage side is acting as a motor, while the high voltage side is acting as a generator with an inductive load coupled.

The extended voltage equation (3.1) that describe the electric circuit presented in Fig. 3.3 can be written as:

$$E_H = (R_H + \frac{d}{dt} L_H) \cdot I_H + \frac{d}{dt} M \cdot I_L + V_H \tag{3.3}$$

$$V_L = (R_L + \frac{d}{dt} L_L) \cdot I_L + \frac{d}{dt} M \cdot I_H + E_L \tag{3.4}$$

3.2 FEM formulation for coreless machines

FEM has become a standard method for modeling electrical machines. The differential field equations that govern the magnetic field phenomena are:

$$\nabla \times H = J \tag{3.5}$$
$$\nabla \cdot B = 0 \tag{3.6}$$
$$\nabla \times E = -\frac{dB}{dt} \tag{3.7}$$

where H is the magnetic field, J is the total current density, B is the magnetic flux density, and E is the electric field. A more extensive description of the FEM equations may be found in [47].

The problem is usually addressed with a representative 2D geometry in order to reduce the computation demands of FEM. Radial flux machines has an invariant axial cross section. Full 3D simulations are required in axial flux machines and other complex geometries without a significant section. The Department for Electricity has been developing 2D FE methods for electric machines calculation with outstanding results in many projects. Unfortu-

nately these previous experience could not been use for axial flux topologies so a completely new approach was required.

The solution has to describe the behavior of the machine with time. 3D time domain solutions require long computation time and some commercial programs like COMSOL do not support this feature and they are usually avoided. The method used here take advantage of the coreless configuration of the machine under investigation to simplify the equations. A static 3D FEM analysis of the magnetic field with the proper processing is enough to solve the problem. The method is applicable to toothless machines, both cored and coreless, and has been previously implemented for 2D field solutions [48]. The magnetic field in the air gap only depends on the position of the rotor and not to the relative position between the rotor and the stator teeth if the stator has no teeth that perturb the magnetic field. The time dependent magnetic field z component can be expressed as

$$B_z(\theta, r, z, t) = B_z(\theta, r, z, \theta / \omega) \tag{3.8}$$

With this change of variables, the emf can be obtained with space integration instead of time domain integration. The emf for a single conductor is therefore calculated according to

$$E(t) = -\frac{d}{dt}\lambda_M = \int B_z \cdot \omega \cdot r(l) \cdot dl \tag{3.9}$$

where r can be a 3D function that defines the geometry of the coil including the end-winding. The expression is integrated along a complete phase winding, including the end region. B_z is derived from a 3D FEM static simulations. The line parameters that define the machine, resistance and inductance, are calculated independently and applied in equations (3.3) and (3.4).

3.3 Losses in the motor/generator

Electric machines are complex systems subjected to different physic phenomena. Losses originate from the combination of different loss mechanisms that can not be measured independently. The losses in electric machines may be classified as:

Fluid dynamic forces

Drag losses are a non liner problem derived from the Navier-Stokes equations. A first approximation to the problem is considering drag losses proportional to the cube of the rotational speed. This is true for a range of

speeds where the Reynolds number is assumed constant and for the same turbulence flow regime [49]. The friction of a rotating cylinder can be calculated as

$$P_{drag} = C_f \cdot \rho \cdot \pi \cdot r^4 \cdot l \cdot \omega^3 = k_{drag} \cdot \omega^3 \qquad (3.10)$$

where C_f is a dimensionless friction coefficient dependent of the Reynolds number, ρ is the air density, r and l are the cylinder radius and length, and ω stands for the rotational speed. The air friction has also a positive effect in the heat flow. Operation in a low atmosphere pressure reduces the losses but eliminates the necessary convection heat flow. Controlled atmospheres with mixtures of air, helium and SF_6 have been tested with positive results [50] and [51].

Mechanical losses

The rotor rests on the stator with bearings and seals. The friction between both surfaces is a complex tribology problem out of the scope of this thesis. At a first approximation, mechanical losses can be considered proportional to the speed for the load and speed range of the machines studied [52]. Magnetic bearings are more suitable for high speed flywheels and the losses are considered independent of the speed. In this thesis the bearing losses are studied with:

$$P_{bearing} = k_{bearing} \cdot \omega \qquad (3.11)$$

Joule losses

The Joule effect refers to the heat generated in a conductor by the current flowing through it. It applies to the stator currents and to excitation currents, both in IM and SB machines. The losses are not proportional to the speed but to the phase current and resistivity, and can be expressed as:

$$P_{bearing} = 3 \cdot R \cdot I^2 \qquad (3.12)$$

Eddy current losses

The eddy current losses are a form of Joule losses. When a variable magnetic flux is linked to a conductor, a voltage is induced. The iron in the stator, the copper windings and the magnetic material are conductors and react as a short circuit against the induce voltage with the so called eddy currents. The currents are not uniform through the conductor mass but rather concentrated in the surface of the conductor in a region confined in the skin depth:

$$\delta = \sqrt{\frac{2 \cdot \rho}{\omega \cdot \mu_0 \cdot \mu_r}} \tag{3.13}$$

The skin depth δ in ferromagnetic materials at 50 Hz is less than half mm. The mesh required to solve this problem with FEM is several orders of magnitude smaller than for the rest of the machine and becomes a complex numerical problem. Analytic methods are still preferred in this field.

The losses are greatly reduced when the conductor is thinner than the skin depth. This is the reason why the stator is made with laminated steel and the lamination thickness b is thinner for high speeds machines. Under this premise the problem becomes linear and the eddy current losses can be calculated for plates and cylinders as:

$$P_{eddy,plane} = \frac{B^2 \cdot b^3 \cdot l}{3 \cdot \rho} \cdot \omega^2 \tag{3.14}$$

$$P_{eddy,cylinder} = \frac{\pi \cdot d^4 \cdot B^2 \cdot l}{32 \cdot \rho} \cdot \omega^2 \tag{3.15}$$

The eddy current losses in plane are calculated as part of the iron losses. The analytic solution is applied only in the conductors. The magnetic field peak B is obtained in the radial and axial components with 3D simulations. The fourier series of the magnetic field is used to calculate the losses due to each harmonic. The magnetic field over the conductors in slotted stators is very small because they are shielded by the steel. In coreless machines, the absence of iron in the stator increases the eddy current losses in the windings and it can become the main loss mechanism.

Permanent magnet material is usually thicker than their skin depth which may present complex geometries and render analytic solutions unviable. Electromagnetic FEM simulations are required to solve this problem as presented in Paper VII.
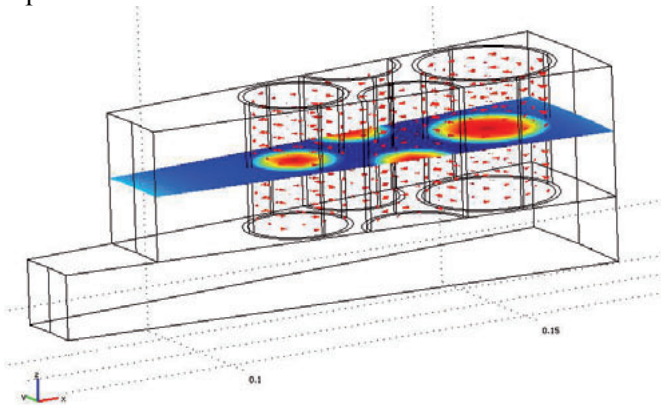

Figure 3.4 Section of a radial flux machine rotor with the eddy currents induced in the magnets represented with arrows obtained with a FEM model. The slide shows the magnetic field distribution created by the eddy current losses.

Iron losses

The losses in the iron are significant in the stator core and in the rotor poles. Iron losses produced by several interconnected and complex effects. The hysteresis losses appear when the atomic dipoles align themselves with an external field. Soft magnetic materials like silicon steel or ferrite in small motors are used due to the lower hysteresis losses. They may be estimated with the empirical relation:

$$P_h = k_h \cdot B^{k_s} \cdot \omega \qquad (3.16)$$

where k_s is the Steinmetz coefficient and varies from 1.5 to 2.5 depending on the material but usually set to 1.6. The hysteresis losses are completed with the excess losses. The internal structure of the laminated steel is made up of domains which borders move under the influence of the external field. The phenomena is called Barkhausen jumps [53] and it introduces further loss in the process, that has been experimentally estimated with:

$$P_e = k_e \cdot (B \cdot \omega)^{1.5} \qquad (3.17)$$

Eddy currents are also acting in the surface of the steel, following eq. (3.14), causing a reduction in the magnetic field. The parameters are calculated with a curve fitting from the losses given by the steel manufacturer. The magnetic field in an electric machine is less homogeneous than in the standard test for laminated steel and a factor is usually added varying from 20% [54] to 50% [55]. The uncertainty of estimation increases when the steel is saturated over the manufacturer's data and extrapolation is needed. This discrepancy is also due to the so called rotational losses [56] and the stray losses. The stray losses are eddy current and hysteresis losses in the armature surrounding iron due to undesired and sometimes not calculated flux leakage.

The calculation of iron losses in the rotor requires a different approach. The variation of the magnetic field is produced mainly by the slot ripple. The frequency depends on the number of slots per pole and phase and the shape of the poles. The fundamental harmonic is the number of slots times the rotational speed. The skin depth is uncertain due to the non linearity of the iron permeability and the high order harmonics content. The magnetic field reaches the rotor poles in the radial direction and is evenly distributed in the steel in the tangential direction in a path confined in only a few millimeter layer The tooth ripple losses are produced mostly by the magnetic field that flows in the tangential direction in the surface of the rotor rather than the radial magnetic field [57]. The high gradients in the magnetic field create a numerical complexity that makes FEM less applicable [58]. Instead, several semi-empiric methods have been proposed. The approaches of seven authors

are compared in [59]. The author has calculated the tooth ripple losses for a given example with [57], [60] and [61] approaches with similar results although the last one is easier to implement in variable speed operation.

Hysteretic losses are negligible compare to eddy current losses in solid poles. When lamination of the rotor is not possible, mechanization of grooves in the pole is an option to reduce losses. Values of 0.5 to 0.9 W/cm^2 can be used as a thumb rule [57].

It is possible to solve the problem with a FEM model if the machine rotates slowly so that the mesh is finer than the skin depth. A machine has been modeled at 500 rpm. The convergence of the problem required some assumptions; the permeability remains constant in a small layer in the surface. Gibbs and Oberretl obtain an equivalent permeability through tables while Lawrenson gives reference values. A relative permeability of 150 is used considering these authors suggestions and the saturation curve. A distinction of two regions with different μ_r is done because the reduction of μ_r in such a small region does not affect the reluctance of the magnetic circuit. The machine characteristics are defined in Section 5. The current distribution in the rotor pole follows the pattern anticipated by Oberretl as presented in Fig. 3.5. There is a region where the current change from negative to positive over the same radius as the magnetic field which induces the current is transversal.
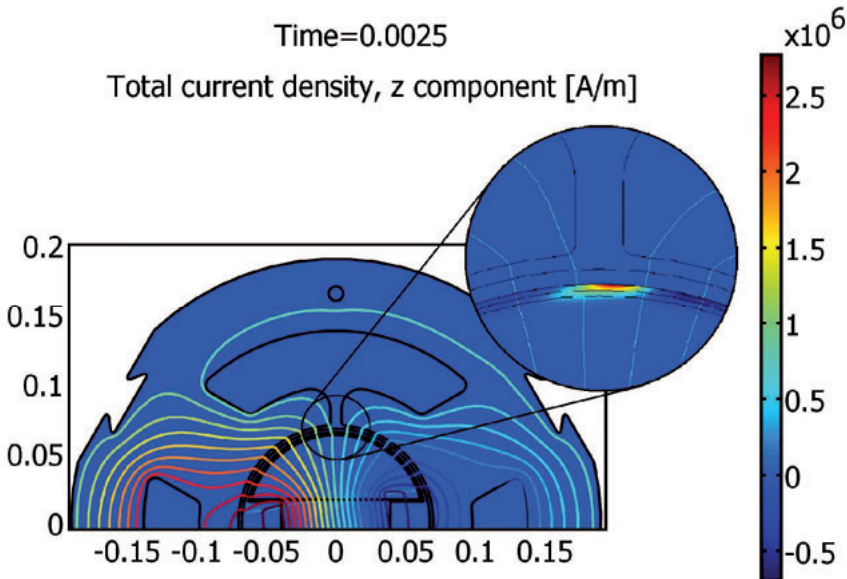

Figure 3.5 Current distribution in a salient pole at 500 rpm. Observe that the current changes from negative to positive over the radius in a certain region of the skin depth.

A hybrid method to calculate the eddy current losses in salient poles is proposed. First the losses at low speed are calculated with FEM simulations. FEM simulations give the harmonic content and the armature reaction. The harmonic content is independent of the speed. Then the losses at high speed are extrapolated at high speed considering the losses proportional to $\omega^{1.5}$. It can be argue that the saturation is poorly taken into account as previous authors. The improvement is that the harmonics and current distribution are trustworthy and the permeability is estimated based on previous empirical analysis. The method has been validated with experimental data and results are presented in Paper IX.

3.4 Efficiency determination under variable speed operation

Variable speed machines, as their name indicate, operate in a rage of speeds and power and therefore have not a nominal efficiency. They are characterized by a map of efficiencies as presented in Fig. 3.6.
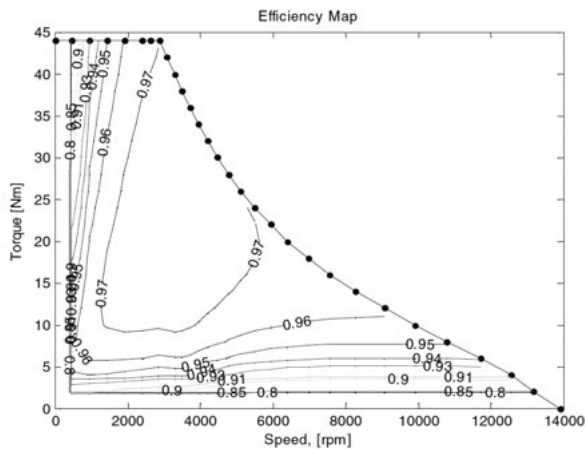

Figure 3.6 Map of efficiency of a PM motor. Figure reprinted from [62].

The losses presented in Section 3.3 are dependent on the frequency and phase current. Strictly speaking, the dependency on the phase current implies the efficiency of the motor to depend on the control strategy of the driver. V/f scalar control requires higher currents than a vector control which gives the highest torque to current.

The efficiency of the motor depends on the feed voltage. Stationary machines are powered by the grid at constant voltage. However electric vehicle motors as powered by batteries that reduce their voltage with the State of Charge (SoC). Reductions of 10% in the efficiency have been reported at low SoC [63]. The driveline presented has a constant DC in the high power side which powers the traction motor preventing this efficiency drop.

The optimal motor has high average efficiency at the operational regime rather than high peak efficiency at an unrealistic working point. There are several standard drive cycles used to determine the speed and torque at every time. The combination of the efficiency map and the power requirements from a drive cycle give the average efficiency of an electric motor.

3.5 Thermal analysis

Losses in electric machines represent a heat source. Heat may be transfer by means of conduction, convection and radiation. The equations that apply to these three phenomena are:

$$Q = -k \cdot \nabla T \qquad (3.18)$$

$$Q = h \cdot A \cdot (T_s - T_a) \qquad (3.19)$$

$$Q = e \cdot \sigma \cdot A \cdot (T_s^4 - T_a^4) \qquad (3.20)$$

Where k is the thermal conductivity of the material, h is the heat transfer coefficient between a surface and air, A surface area, T_s and T_a are the surface temperature and the ambient temperature, e is the emissivity and σ is the Stephan-Boltzmann constant [64]. The heat transfer coefficient is the most problematic parameter in the calculation. It depends on the air flow and the calculation requires complex fluid dynamic simulations. The heat transfer coefficient h also depends on the surface characteristics, so experimental data is always required [65]. Good estimations can be made with tabulated values. Correlations of h are found in [66], [67] and thermal properties of electric machine components are presented in [67]. Heat flux by radiation at standard temperatures is much lower than convection and therefore is usually neglected.

4. Test results

> And that prince who bases his power entirely on...words, finding himself completely without other preparations, comes to ruin.
>
> Niccolo Machiavelli.

4.1 Axial Flux, Single Wounded prototype (AFSW)

An available axial flux coreless machine has been simulated and tested to validate the simulation methods presented in Section 3.2 and the loss mechanisms model presented in Section 3.3. The machine is a small-scale three-phase AFPM with a coreless winding sandwiched between two rotor discs. The machine topology is described in Table 4.1 and presented in Fig. 4.1.

Table 4.1.

AF simple wounded prototype characteristics.

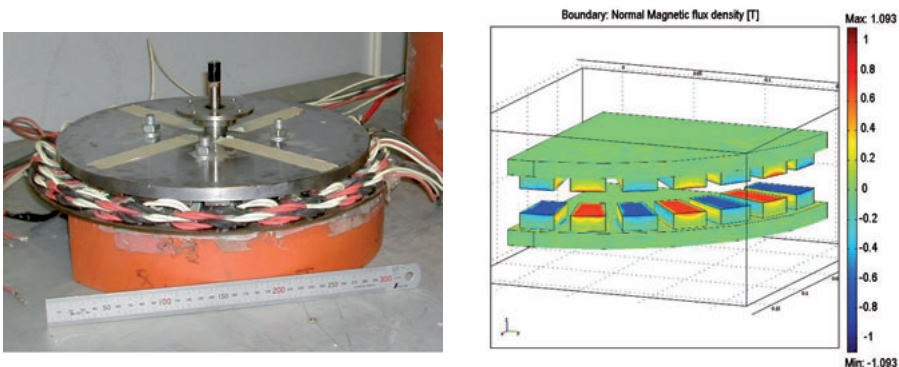|	
Rotor outer radius (mm)	150
Rotor inner radius (mm)	110
Air-gap length (mm)	16
Number of pole pairs	14
PM height / average width / length (mm)	10 / 20 / 40
B_r of the NdFeB PM (T)	1.2
Total number of magnets	56
Outer diameter of cable (mm)	3.35
Cross section area of the cable (mm^2)	2.5
Number of strands	50

Figure 4.1. Machine view and simulated magnetic flux density in the air gap.

The AFSW machine has been simulated with both 2D and 3D FEM models and the results has been compared in Table 4.2. End winding effects in machines with high air gaps are usually not negligible. The magnetic field in the air gap from 2D simulations has higher content of harmonics than in 3D simulations and measurements, which leads to different values of estimated eddy current losses.

Table 4.2.

Content of harmonics in the induce emf for the trapezoidal pole configuration.

Harmonic	2D	3D	Experimental
3rd	0.63%	0.24%	0.46%
4th	0.03%	0.16%	0.13%
5th	0.35%	0.23%	0.18%
6th	0%	0.09%	0.13%

The losses in the AFSW machine have been calculated with several spin down tests [68]. The machine was accelerated and then left to deceleration by its own friction at different air pressure. The drag losses at low air pressure are neglected, so the drag losses at atmospheric pressure are obtained by subtracting the total losses. The idea behind the spin down test comes from a simplified form of the so called synthetic load method [69].

The losses are calculated for each speed by the derivative of the speed. The high inertia of the rotor compare to the losses ensures a quasi static variation of the speed. The losses can be calculated with:

$$P = \frac{dE}{dt} = \frac{d(1/2 \cdot I \cdot \omega^2)}{dt} = I \cdot \omega \cdot \frac{d\omega}{dt} \qquad (4.4)$$

The machine was accelerated up to 850 rpm (200 Hz$_e$). The measured and modeled losses presented in Fig 4.2 show the agreement obtained. The measured eddy current losses are 1.79 W while calculations give 2.56 W.
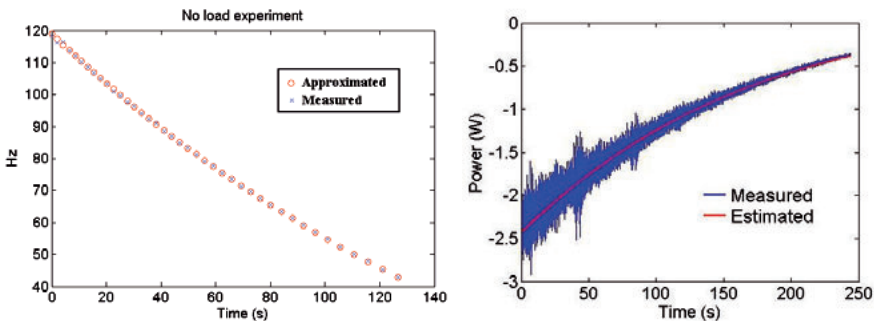

Figure 4.2. Spin-down test measurements and estimations for the speed and losses.

4.2 Axial Flux, Double Wound prototype (AFDW)

An Axial Flux Double Wound (AFDW) machine i. e. with two sets of three phase windings has been designed and constructed. The mechanical analysis determined that solid permanent magnets are too brittle so poles are segmented in several round magnets as presented in Fig. 4.3. This topology is common in high speed axial flux machines [70].

Axial flux geometries are more favorable for high number of poles due to the high end winding region in the outer diameter and better magnetic field distribution in the air gap. On the other hand high frequency operation increases stator losses and switching losses associated to power electronic converters. Concentrated windings reduce the end windings but require high number of poles. A nominal speed of 20,000 rpm is reached with 12 poles in [70], 8 poles in [71], and 8 poles and 50,000 rpm in [72]. A compromise of 6 poles has been selected for the AFDW prototype. Parameters are presented in Table 4.3.

Table 4.3.

AFDW prototype parameters

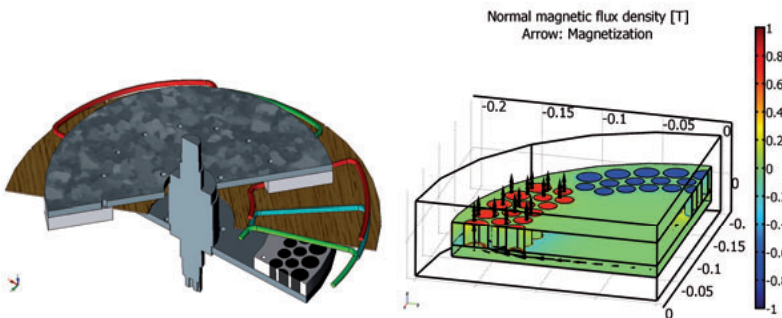|	
Rotor outer radius (mm)	160
Rotor inner radius (mm)	110
Air-gap length (mm)	30
Number of pole pairs	3
PM height / arc / length covered	20 mm / 54º / 50 mm
Region covered by magnets	60%
B_R of the PM (T)	1.3
Number of magnets per pole	17
Outer diameter of cable (mm)	4.05
Cross section area of the cable (mm^2)	4.0
Number of strands	56
Number of turns per phase and pole	4 / 12

Figure 4.3. Axial flux machine representation and magnetic field in the air gap.

The peak voltage has been calculated with the method proposed in Section 3.2 with an error of 1.5% and the third harmonic discrepancy from 11.1% measured to 12.2% calculated.

The magnetic flux distribution shows irregularities due to the segmented pole topology as seen in Fig. 4.4. The magnetic flux has been considered as two superposed functions in the calculation of the eddy current losses in the windings. One of the functions represents the main and principles harmonics and the second is the superposition of the ripple produce by the magnets with frequencies proportional to the distance between magnets. Further explanation is found in paper V.
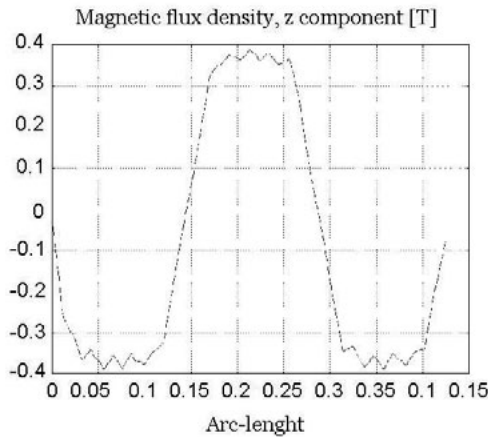

Figure 4.4. Magnetic field density at average radius for a split magnet shape.

Eddy currents in the magnets are usually induced by space harmonics. The AFDW prototype is coreless, so eddy current losses are only induce by time harmonics, i. e, the harmonic content of the stator currents from the inverter. A time-harmonic 3D FEM model, presented in Fig. 3.4, has been developed to estimate these losses. The harmonic content in the current has been implemented in the model with data from simulations and experimental measurements. It has been conclude that the losses induced in the magnets are negligible and there is no risk of demagnetization due to local heating, due to the low inductance of coreless machines. The study is presented in Paper VII.

A double wound machine is part of an electric driveline presented in Fig. 1.3. Test results with a traction motor following a drive cycle are not available for publication yet. The presented tests consist of a DC power source and a DC/AD drive couple to the low power side and a diode rectifier bridge and a variable resistance couple to the high power side. The test lay out is presented in Fig. 4.5.
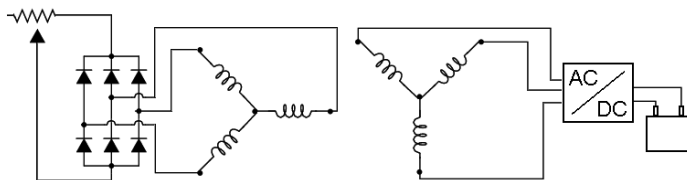
Figure 4.5. Test set up. The DC source, connected to a PCS, delivers power to the Low Power side of the TVLM. The emf inducer in the High Power side is connected to a bridge rectifier and power is consumed in a variable resistance.

During the test, the variable resistive load changes with time, extracting power from the system. The power flow in the system is presented in Fig. 4.6. The power extracted from the high power side suffers rapid changes while the power deliver by the low power side remains almost constant. The power flow in the low power side depends on the control of the PCS and can be smoothed even more if required. The difference between the power extracted and delivered by the power source is balanced by the kinetic energy of the TVLM rotor, acting as a flywheel. Fig. 4.6 (b) shows how the speed and energy evolves. The energy is proportional to the square of the speed.
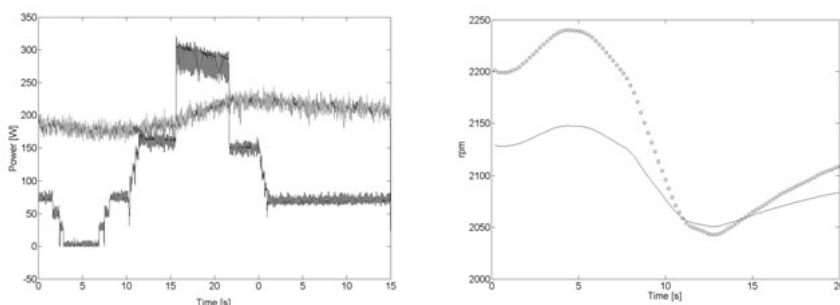

Figure 4.6. (a) Power extracted in the High Power (black) and in the Low Power side (grey).(b) Speed and kinetic energy (out of scale) of the flywheel.

4.3 Radial flux coreless prototype

The purpose of the new prototype is to test the radial coreless configuration and create a machine to demonstrate the complete driveline. Fig. 4.7 shows the configuration of the prototype where (1-4) are the rotating elements, (5) is a ball bearing, and (6-8) are static parts. The rotor consists of a hollow aluminum part (1) which supports a six pole Halbach magnet array (2). A magnetic back yoke (3) rotates synchronously with the rotor to eliminate eddy current losses in the return path of the magnetic flux. The rotor Gravity loads are supported with passive magnetic bearings (4 and 6). The stator is

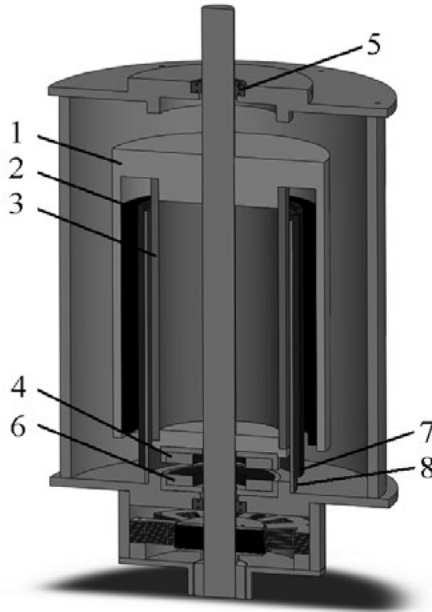made with two sets of concentrated windings (7) placed on a non magnetic and non conductive cylinder (8).

Fig. 4.7. Description of the radial flux coreless prototype.(to be improved)

The number of poles is again set to six after an optimization process which is in agreement with other authors [73]. Concentrated windings are chosen over distributed windings, even for induced voltage of about 40% less, based on previous experiences in the end winding region. The schematic is presented in Fig. 4.8. The windings overlap would exceed the air gap and intersect with the rotor if distributed windings were selected.
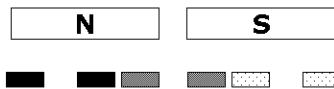

Fig. 4.8. Concentrated winding representation over one pole.

Taps in the prototype allow Δ and Y connections to change the phase voltage. This allows operation in different drivelines configuration. The same design can be use to insert a flywheel in a small commercial electric vehicle and in custom drive lines. Case M (for mopped) uses the voltage levels of the battery and electric motor of an electric mopped. Case D (for drive line) sets a high trans-former ratio between battery and traction motor to increase the efficiency of a test drive line. The DC to V_{rms} relation is esti-

mates as 0.48 from the previous FW experience. The driveline parameters of the driveline in both con-figurations are presented in Table 4.4.

Table 4.4.

Voltage parameters of the RFCM for different configurations (to be im-proved)

M case / Low Voltage		D case / Low voltage	
NLP/NHP	4/10	NLP/NHP	4/10
L (m)	0.2 m	L	0.2 m
Connections	Y/Δ	Connections	Δ/Y
Max rpm	3,000	Max rpm	12,500
E line rms	25/35 V	E line rms	58/260 V
V (DC)	60 V	V (DV)	100 V

The stator is winded with 3.14 mm² Litz wire composed of 100 strands of 0.20 mm. of diameter. Outer diameter is 2.80 mm. The back emf induced is obtained with a FEM simulation; for radial configurations 2D FEM models are suitable. The results are presented in Fig. 4.9.
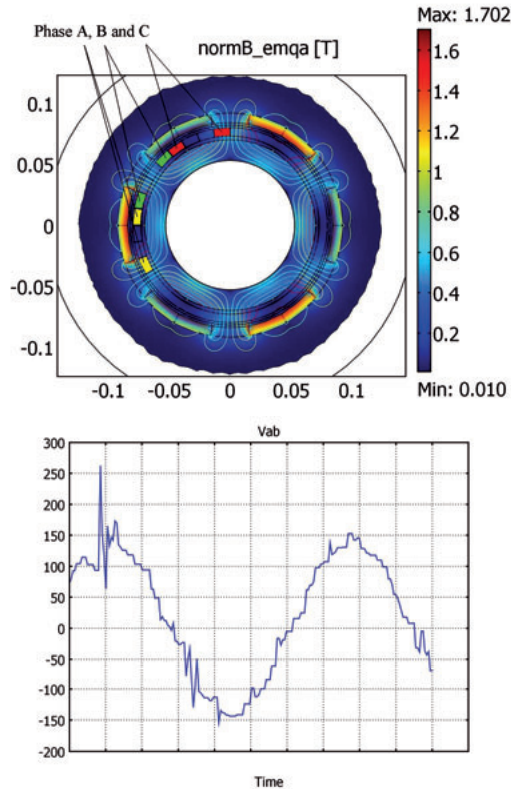

Fig. 4.9. Magnetic field distribution and back emf.

5. Electric motors for vehicles

> I think there is a world market for maybe five computers.
>
> Thomas Watson, chairman of IBM.

5.1 Motor prototype

An electric motor has been designed and partially constructed. The investigation of electric motors is part of a wider project. The goal is to convert a vehicle with a conventional IC motor into a full electric vehicle. A new design, rather than buying a commercially available motor, was developed to increase the understanding of operation and to investigate possible improvements based on a scientific approach. The specifications required are presented in Table 5.1.

Table 5.1.

Traction motor specifications

Power	40 kW
Poles	2
Max. speed	6,000 rpm
DC Voltage	400 V

Preliminary estimations presented in Table 5.2 shed light to the magnitude of the challenge and helps to size the system:

Table 5.2.

Motor parameters first approach

Parameter	Estimation	Value
AC_{rms} line voltage	DC Voltage x 0.65	230 V
Rotor radius max.	FEM mechanics	100 mm
DC current	P = V x I	100 A
L max.	$V = R_L \cdot I + \dfrac{d}{dt} L \cdot I + E$	20 mH
E		200 V

The geometry adopted is presented in Table 5.3.

Table 5.3.

Motor parameters adopted

Rotor radius	65 mm
Active rotor length	240 mm
Air gap	5 mm
Turns per phase	16
Back emf	195 V
Phase inductance (d-q)	1.7 - 2.5 mH
Phase resistivity	7.5 mΩ

Concentrated windings

Concentrated windings are physically shifted 120º in two pole motors and are a good educational instrument to visualize the magnetic flux distribution in a three phase stator. Construction is also made simpler and more compact than distributed windings. Concentrated windings are also better suitable for solid pole rotors as the slot harmonic frequency decays significantly. Distributed windings may require 48 slots while the chosen design has only 3. The stator is made with M300-35A steel plates.

The scientific discussion on winding design concluded hundred years ago in favor of distributed windings because of the better magnetic field distribution and the lack of pole shoes. Concentrated windings have thick pole shoes which increase the outer diameter of the stator and consequently the magnetic flux path.

Rotor

The rotor geometry consists on a hexahedral magnet sandwiched between two solid steel half cylinders. The rotor is held together with two circular plates attached to the edges of the rotor as seen in Fig. 5.1. This geometry is compact and robust, although some drawbacks are encountered. There is less space for magnetic material, as the length of the magnets placed on the rotor's diameter is π times less than in peripheral surface arrangement. The geometry limitations do not apply for motors as the magnetic flux density at no load in motors is lower than for generators. It should also be noted that the rotor has a negative saliency.
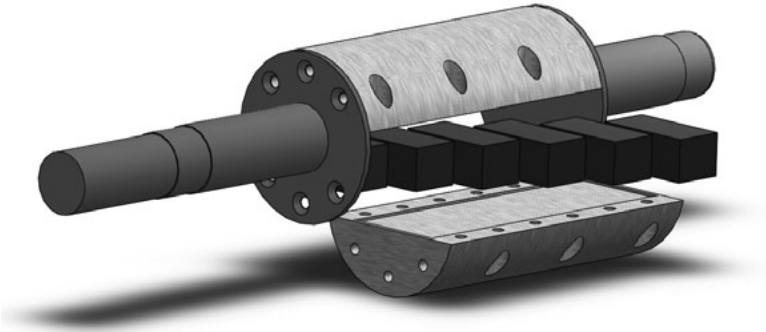
Figure 5.1. Rotor geometry consisting of hexahedral magnets between two solid steel half cylinders. Exploded diagram.

5.2 Losses

The losses are calculated as presented in Section 3.3. The losses at full load and 6,000 rpm are summarized below.

Fluid mechanic losses

Fluid mechanic losses are estimated approximating the rotor to a perfect cylinder with the friction coefficient *Cf* [49] and with eq. (3.10). The drag losses usually refer to the fan, as the drag losses in the rotor are negligible. At 6,000 rpm the losses are barely 10 W.

Friction losses

Bearing losses depends on the radial and axial forces. With an elastic coupling to the shaft the bearing losses are negligible according to the data given by the manufacturer (5 W).

Joule losses

Joule losses are determined by the current in the stator, which is proportional to the power. For a given voltage, the current is limited by the back emf and the impedance. The electromagnetic power in a three phase salient pole motor is calculated with equation (2.1). The stator current depends also on the control strategy. For each output power a certain load angle maximizes the torque to current ratio. The power is limited to 44.5 kW with a load angle of 108º. At full load the current is approximately 125 A, and the losses according to eq. (3.12) are 350 W.

Eddy current losses

The magnetic field leakage over the conductors is about 4.5 mT. The eddy currents induced by this magnetic field are significant only in machines with solid conductors. The cables are formed with 238 strands of 0.4 mm in diameter. The losses in this case are in the range of one third of mW and can be neglected.

Iron losses

The iron losses in the stator are estimated with a simulation of the magnetic field in the stator. The magnetic field is used as an input to the losses given by the manufacturer. The manufacturer gives the losses at 100 Hz up to 1.5 T; out of this region extrapolation is needed [74]. The losses are estimated to 305 W.

The losses in the rotor are substantially reduced due to the concentrated windings. Using [57] as a reference, the number of stator slots goes from 90 to only 3 although losses are 30 times lower because some other parameters are different. Concentrated winding machines have parameters that are out of range for standard analytic methods. The losses are instead calculated with the FEM method described in Section 3. The FEM model is converged for 250, 500, 750 and 1,000 rpm the results are presented in Table 5.4. The extrapolation of the losses is congruent for the first values and significantly lower at 1,000 rpm. This is explained by the skin depth which is lower for high speed. Thus higher harmonics are lost due to mesh limitations.

Table 5.4.

Losses in the solid pole for different speeds and extrapolation to 6,000 rpm

Speed (rpm)	Losses	$(6,000/rpm)^{1.5}$	Extrapolated losses
250	0.63	117	74.2
500	1.87	41.6	77.7
750	3.47	22.6	78.5
1,000	3.82	14.7	56.2

The losses calculated with Gibb's method, with the limitations presented, are about 50 W [58]. The result of the FEM simulations are therefore self consistent and consistent with analytic solutions. Pending laboratory measurements, 75 W are estimated as pole losses.

Efficiency

The efficiency at a working point is defined as:

$$\eta = \frac{P_{mech}}{P_{tot}} = \frac{P_{mech}}{P_{mech} + P_{Losses}}$$ (5.1)

$$\eta = \frac{44,500 - (10 + 5 + 350 + 305 + 75)}{44,500} = 98.3\%$$

The motor designed is much more efficient than commercially available products so a discussion on efficiency is motivated. The high achieved efficiency compared to commercial machines is attributed to their magnetic field densities over saturation in the iron core. High magnetic density makes the design more compact and light but increases the iron losses. The nominal voltage is also higher than for electric vehicles. High voltage in the battery requires complex electronic circuits to balance the voltage in each cell and manufacturers prefer lower voltages. All the calculations have been done considering a perfect sinusoidal power source. Real systems have a harmonic content that increases the losses, particularly iron losses.

5.3 Thermal analysis

The calculated losses are dissipated to the air following the heat transfers laws presented in Section 3.5. The air flow was unknown as the enclosure could not be designed until measurements of the car were made. The design heat transfer coefficients used are therefore very conservative.

The results presented in Fig. 5.2 shows that the heat transfer of the conductors in contact only with other conductors is poor and the temperature rises over the manufacturer's recommendations. Even though the simulation results are conservative, continuous full load drive would eventually lead to overheating. Water cooling and intensive temperature sensing are proposed. Water hoses intercalated between the conductors would reduce the peak temperature under safety margins.
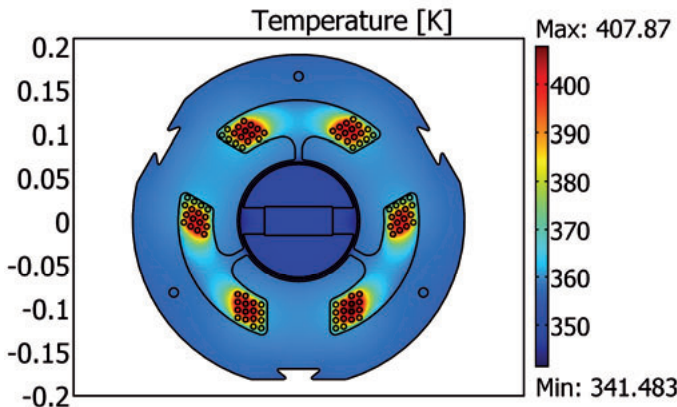

Figure 5.2. Temperature distribution in the motor under nominal speed and power.

6. Discussion

Several prototypes have been constructed to validate the calculation methods and to gain experience in construction techniques. The air gaps of these machines have been intentionally oversized in case the stator becomes out of dimensions in the construction.

The constructed prototypes have performed as expected. Ironless machines can result in more efficient designs despite of their limitations in power rating, as presented in Paper II.

The difference between ironless and slotless machines has been presented for a purpose. Silicon steel is preferred over ferrite because higher saturation limit allows more compact designs. Slotless machines have wide air gaps resulting in low magnetic flux density which makes ferrite cores more attractive. Ferrite has better performance at frequencies up to MHz. The construction experience gained with coreless machines is applicable to machines with ferrite cores due to their similarities.

Electromagnetic problems are very computational demanding. Numerical models require simplifications. Contributions have been presented in the area of coreless machines. Eddy currents in laminated steel and iron are usually calculated with empirical or semi empirical correlations and the magnetic field reaction is always neglected. A method to calculate the eddy current losses in solid poles is presented although it has to be improved to consider the magnetic reaction.

The thesis is focused on numeric methods for motor and generators for electric vehicles although the goal is to improve the overall system, not only separated components. A full driveline with a serial double wound flywheel has been presented and a test bench has been developed.

7. Conclusion

> The power of accurate observation is commonly called cynicism by those who have not got it.
>
> George Bernard Shaw

The present work started at an early stage of the energy storage and electric vehicle research in the Division of Electricity. The research started with an intensive literature review on electric machines for energy storage, electric motors in electric vehicles and electric machines with two sets of windings.

The equivalent circuit of a machine with two isolated sets of windings in the stator has been presented. It has been demonstrated that the predominant flux linkage in the stator windings comes from the rotor magnetic flux while the mutual inductance between both sets of windings has less influence in the performance of the machine. The low mutual inductance in slotless machines makes them suitable for this application.

Numerical methods for coreless machines have been presented and developed. The simulating methods proposed, base on 3D FEM have proven to be time efficient and to perform better than traditional time dependent 2D methods.

The literature review on tooth ripple losses in salient poles shows that conventional analytic methods are neither accurate nor applicable to concentrated winding machines. A new calculating method based on FEM simulations has been presented. The new method has been validated with experimental results and has proved useful.

Simulation of motors with a traditional stator with laminated steel has been addresses. Improved performance for electric vehicle application could be achieved. A two pole machine with a novel rotor topology has been designed and the construction is now ongoing.

Several prototype flywheels have been simulated and constructed. Simulation results and laboratory measurements show good agreement.

The complete driveline for electric vehicles has been demonstrated in a test bench. The concept is ready to be implemented in a full scale vehicle.

Summary of papers

In this chapter, short summaries of the content of the papers are presented and the author's contribution is specified.

PAPER I

Design Parameters Calculation of a Novel Driveline for Electric Vehicles

The paper describes the driveline for electric vehicles based on a motor/generator wounded with two electrically isolated sets of windings (TVLM) with an integrated flywheel. The paper gives an overview of all the components such as power and energy demands, machine control and magnetic bearings characteristics. It also presents some preliminary test results.

The author participated in the description of the equivalent circuit of the machine as well as with experimental work.

The paper is published in the Open access journal World Electric Vehicle Journal, vol. 3, 2009.

PAPER II

Comparison between axial and radial flux PM coreless machines for flywheel energy storage

A comparative study of radial and axial flux topologies for coreless machines is presented. Coreless machines are limited in speed and size with today's magnetic materials; nevertheless the theory is grounded for new expected materials. The theoretical maximum energy product (BH) of $Nd_2Fe_{14}B$ magnet is 120 MGOe. If the development of new magnetic materials continues, the magnetic field in electric machines may increase over the saturation of laminated steel and slotless designs will reach higher power density than slotted machines.

The author wrote the script for the comparison procedure as well as the FEM simulations.

The paper is published in Journal of Electrical Systems, Issue 2, vol. 6, June 2010.

PAPER III

Dual Voltage Driveline for Vehicle Applications.

This journal article presents the equivalent circuit of a TVLM. Machines with two isolated set of windings have not been studied and reported in tech-

nical literature so far. The study is completed with simulations of a drive cycle that shows the response of the system under power transients.

The author contributed with the description of the machine and the simulations both in Dymola and FEM.

The paper is published in International Journal of Emerging Electric Power Systems, vol. 11, issue 3, 2010.

PAPER IV
A Double Wound Flywheel System under Standard Drive Cycles: Simulations and Experiments

In this paper the functionality of a double wound flywheel system is investigated. Different standard drive cycles are applied on the high voltage side to assess the effect of load variations in the system as a whole and particularly in the speed control. The response of the speed control system is investigated with computer simulations. The study is illustrated with experimental results, proving the functionality of the system.

The author participated in describing the equivalent circuit of the motor/generator machine as well as in the laboratory set up.

The paper is published in International Journal of Emerging Electric Power Systems. vol. 11, Issue 4, 2010.

PAPER V
3D FEM modeling of ironless Axial Flux Permanent Magnet motor/generators

There are different approaches to model axial flux machines with 2D sections. A simple 3D FEM method is presented based on the special properties of slotless machines. The method is based on a static simulation of the magnetic flux, with makes it less time consuming than time step methods. The paper also discusses the eddy current losses computation, as the main loss mechanism in this kind of machines.

The author played a large role in the writing of the paper.

The paper is published in Journal of Electrical and Electronics Engineering, vol. 4, nr. 1, 2011.

PAPER VI
Losses in Axial-Flux Permanent-Magnet Coreless Flywheel Energy Storage Systems

This paper describes the losses in coreless machines. Main loss mechanisms are identified and optimization strategies are presented. The theoretical studies are validated with experimental tests with good agreement. The eddy current losses are measured through a spin down test.

The author described the loss mechanisms and helped with the experimental set up.

PAPER VII

Filter Influence in Rotor Losses in Coreless Axial Flux Permanent Magnet Machines.

The eddy current losses induced in the rotor magnets are discussed. The losses caused by the magnetic field created by the harmonic content of the stator currents are calculated. The data of the harmonics considered come both from simulations and from laboratory tests. The losses are too low to be measured and compared with simulations. Result implications are discussed.

The author defined the simulations and created the FEM model. Simulations of the inverter to obtain the harmonic content of the currents were performed by coauthors.

PAPER VIII

Electrical Motor Drive-lines in Commercial All Electric Vehicles: a Review

A thorough critical literature review on electric vehicle technologies that includes motor topologies, battery handling active roads is presented. Dynamic drawbacks of in wheel motors are discussed. The paper is completed with a survey on electric vehicles in the market.

The author performed most of the work in this paper.

PAPER IX

Tooth Ripple Losses in Solid Salient Pole Synchronous Machines with Concentrated Windings

A literature review on tooth ripple losses in solid pole machines is presented. Analytic calculations are still the standard method although there is a great amount of synchronous solid pole machines such as claw pole alternators. A FEM procedure is proposed and results are compared with experimental results.

The author has contributed with the literature review and the FEM simulations leading to Fig. 2 and 3.

Svensk sammanfattning

Luftföroreningar i storstäder har diskuterats sedan århundraden. Restriktioner mot uppvärmning med hjälp av kol startade under medeltiden och förordningar om luftkvalitet har bara blivit hårdare sedan dess. Transportsektorn har inte varit främmande för denna tendens, särskilt efter oljekrisen på 70-talet. Debatten om den ekonomiska bärkraften hos elfordon har nu kommit till ett slut, då EU-kommissionen bestämt att konventionella bensinbilar kommer att tas bort i städer år 2050.

Elfordonsteknik är ett tvärvetenskapligt ämne i ständig utveckling. Det saknas en överenskommelse om en standard konfiguration för drivlinan och forskningen pågår fortfarande. På samma sätt väljer varje biltillverkare sin egen elmotortopologi för de elbilar som finns på marknaden idag. Det finns heller ingen standard för motortopologi, även om elmotorer inte genomgått någon större förändring sedan utvecklingen av neodymiummagneter med hög koercivitet för trettio år sedan. Det finns marginaler för förbättring av den magnetiska fältstyrkan och Avdelningen för Ellära vid Uppsala universitet gör betydande forskning inom området. Denna avhandling undersöker numeriska lösningar för elektriska maskiner för fordon, både i drivlina och i drivmotorn.

Kapitel 1 presenterar en drivlina med två galvaniskt isolerade spänningsnivåer. En lågeffektsida drivs med optimal spänning med avseende på batteridrift, medan en högeffektsida drivs med en högre spänning för att optimera drivmotorns verkningsgrad. Sidorna är ihopkopplade med hjälp av ett svänghjul som stabiliserar de effekttransienter som uppstår under en körcykel. Även batteriekonomi och en litteraturforskning om svänghjul presenteras.

En utredning om topologier hos elektriska maskiner för elbilar presenteras i kapitel 2. Den bäst lämpade topologin för vår applikation exciteras med permanentmagneter. Innehållet i detta kapitel är en del av den litteraturstudie om elektriska motorer för fordon och elektriska maskiner för energilagring som presenteras i artiklar.

Kapitel 3 ägnas åt numeriska modeller för elektriska maskiner. Elektriska maskiner med två uppsättningar av spolar beskrivs med en ekvivalent krets. De nödvändiga elektriska parametrarna beräknas med anpassade FEM-modeller. Två viktiga bidrag till numeriska modeller införs. Det första bidraget är en diskussion om maskiner med statorer utan järn, vilket avslutas med en enkel modell för att analysera det magnetiska fältet med hjälp av en sta-

tisk 3D-simulering. Det andra bidraget ägnas åt numerisk beräkning av virvelströmsförluster i fast utpräglade poler. En fullständig beskrivning av förlusterna i elektriska maskiner ger en solid grund för vidare diskussion om verkningsgrad.

Kapitel 4 presenterar experimentella resultat från prototyper som har konstruerats för att validera de teoretiska modeller som presenteras i tidigare avsnitt. Den första prototypen består av en elektrisk maskin med axiellt flöde och enkelt lindning. Den andra har axiellt flöde, men dubbel lindning,. Den tredje prototypen har dubbel lindning och radiellt flöde.

Kapitel 5 fokuserar på drivmotorer för elfordon. En prototyp för att studera konstruktions- och beräkningsprocess om teorin om förluster och de numeriska metoder som presenteras i Kapitel 3 tillämpas.

Acknowledgment

References

[1]   Lynette Cheah and John Heywood, "The cost of vehicle electrification: a literature review", Sloan Automotive Laboratory, Massachusetts Institute of Technology, MIT Energy Initiative Symposium, April 8, 2010, Cambridge, Massachusetts.

[2]   European Commission, "Environment fact sheet: moving towards clean air for Europe", 2006.

[3]   Rural Development, Natural Resources and Environment Management Unit, East Asia and Pacific Region, The World Bank, "Cost of Pollution in China: Economic Estimates of Physical Damages", February, 2007, Retrieved from http://siteresources.worldbank.org/INTEAPREGTOPENVIRON-MENT/Resources/China_Cost_of_Pollution.pdf, August 2011.

[4]   European Commission, "White Paper: Roadmap to a Single European Transport Area – Towards a competitive and resource efficient transport system," Brussels, 28.3.2011

[5]   S. Pathak and R. Prakash, "Development of High Performance AC Drive Train," in Electric and Hybrid Vehicles, 2006. ICEHV '06. IEEE Conference on, 2006, pp. 1-3.

[6]   Christopher, D.A. and Donet, C., "Flywheel technology and potential benefits for aerospace applications", Proceedings Aerospace Conf., vol. 1, pp:159 - 166 Aspen, CO, USA, 21-28 March 1998.

[7]   Kato, S., Takaku, T., Sumitani, H., and Shimada, R., "Development of voltage sag compensator and UPS using a flywheel induction motor and an engine generator", Electrical Engineering in Japan, vol. 167, n. 1, pp. 74-81, 15 April 2009.

[8]   Matthew L. Lazarewicz and Alex Rojas, "Grid Frequency Regulation by Recycling Electrical Energy in Flywheels", 38th Annual Frontiers of Power Conference, Proceedings, Stillwater, Oklahoma, USA 2005.

[9]   Dong-Jing Lee; Li Wang, "Small-Signal Stability Analysis of an Autonomous Hybrid Renewable Energy Power Generation/Energy Storage System Part I: Time-Domain Simulations", IEEE Trans. on Energy Conversion, Vol. 23, Issue 1, Pages:311 – 320, March 2008.

[10]   Harvey Glickenstein, "Electric trams without the wires", IEEE Vehicular Technology Magazine, v 1, n 4, p 50-54, December 2006

[11]   B. Bolund, H. Bernhoff and M. Leijon, "Flywheel energy and power storage systems", Renewable Sustainable Energy Rev 11, 2007.

[12]   M. A. Rahman, A. Chiba, and T. Fukao, "Super high speed electrical machines - summary," in IEEE Power Engineering Society General Meeting, Vol. 2, pp: 1272-1275, Denver, CO, USA 2004.

[13]   Post, R.F., Fowler, T.K., Post, S.F., "A high-efficiency electromechanical battery" Proceedings of the IEEE Volume 81, Issue 3, March 1993.

[14]   Mason, L.S., and Oleson, S.R., "Spacecraft impacts with advanced power and electric propulsion", IEEE Aerospace Conference Proceedings, Big Sky, Montana, USA, March 2000.

[15]   Active Power. Retrieved August 2011: http://www.activepower.com/economically-green/.

[16]   Caterpillar. Retrieved August 2011: http://www.cat.com/power-generation/ups.

[17]   Pentadyne. Retrieved August 2011: http://www.pentadyne.com/

[18]   Lazarewicz, M.L., and Rojas, A., "Grid frequency regulation by recycling electrical energy in flywheels", Proceedings of the IEEE PES General Meeting, Denver, Co, USA.2004.

[19]   I. J. Iglesias, J. C. Martinez, M. Lafoz. "A Kinetic Energy Storage System for Railways Applications." World Congress on Railway Research, Seoul, Korea 2008.

[20]   Anton Mittereggera, Gerhart Penninger, "Austrian pumped storage power stations supply peak demands", World Pumps, Vol 2008, Issue 500, May 2008.

[21]   "Gyrobus: a great idea takes a spin." Retrieved August 2011: http://photo.proaktiva.eu/digest/2008_gyrobus.html.

[22]   Hearn, C.S., Flynn, M.M., Lewis, M.C., Thompson, R.C., Murphy, B.T., and Longoria, R.G., "Low Cost Flywheel Energy Storage for a Fuel Cell Powered Transit Bus", IEEE VPPC 2007. Vehicle Power and Propulsion Conference, Arlington, TX, USA2007.

[23]   U. Henning1, F. Thoolen, M. Lampérth, J. Berndt, A. Lohner, and N. Jänig, "Ultra low emission traction drive system for hybrid light rail vehicles", International Symposium on Power Electronics, Electrical Drives, Automation and Motion, SPEEDAM, Taormina, Italy 2006.

[24] Briat, O., Vinassa, J.M., Lajnef, W., Azzopardi, S., and Woirgard, E., "Principle, design and experimental validation of a flywheel-battery hybrid source for heavy-duty electric vehicles", Electric Power Applications, IET, Sept. 2007.

[25] Flywheel Energy Systems Inc., "Performance Verification of a Flywheel Energy Storage System for Heavy Hybrid Vehicles. Rev. A, Whitepaper", Retrieved from http://blueprintenergy.com/ Downloads/2010-0121%20Performance%20verification.pdf, August 2011.

[26] John M. Miller, Michael Liedtke, Bobby Maher, and Juergen Auer, "Ultracapacitor Energy Storage Systems of Heavy Hybrids: A Sustainable Solution", EVS-23, The 23rd International Battery, Hybrid and Fuel Cell Electric Vehicle Symposium & Exposition, Anaheim, California, USA 2007.

[27] Paul P. Acarnley, Barrie C. Mecrow, James S. Burdess, J. Neville Fawcett, James G. Kelly, and Philip G. Dickinson, "Design Principles for a Flywheel Energy Store for Road Vehicles", IEEE Trans on Ind. Appl., vol. 32, no. 6, Nov/Dec1996.

[28] X. Liu, D. Diallo and C. Marchand, "Design methodology of fuel cell electric vehicle power system", IEEE International Conference on Electrical Machines, Villamoura, Portugal, 2008.

[29] J. Fenton and R. Hodkinson, Lightweight Electric/Hybrid Vehicle Design: Automotive Engineering Series, Chapter 1: Current EV design approaches, Elsevier Butterworth-Heinemann, 2000.

[30] Maria Blomberg, Super premium efficiency synchronous motor and drive package Taking energy efficiency to a new level, ABB201103152ENG Rev, GPG Serial OEM Motors, March 2011.

[31] Rault, "The 2010 Paris Motor Show, press release", Paris, France, September 30, 2010.

[32] G. Friedrich, "Comparative study of three control strategies for the synchronous salient poles and wound rotor machine in automotive applications with on board energy," Power Electronics and Variable-Speed Drives, Fifth International Conference on, , pp. 706-709, London, UK 1994.

[33] Ofori-Tenkorrang, J., Lang, J.H., "A Comparative Analysis of Torque Production in Halbach and Conventional Surface-Mounted Permanent-Magnet Synchronous Motors", Conference Record of the 1995 IEEE Industry Applications Conference 30th IAS Annual Meeting, Orlando Florida, USA.

[34] M. A. Rahman and M. A. Masrur, "Advances on IPM technology for hybrid electric vehicles," IEEE Vehicle Power and Propulsion Conference, pp. 92-97, VPPC '09., Dearborn, MI , USA 2009.

[35] Gieras, J. F., and Wing, M., "Permanent Magnet Motor Technology Revised", CRC; 2nd edition (January 15, 2002).

[36] K. B. Ma, Yong Zhang, Y. Postrekhin, and Wei-Kan Chu, "HTS bearings for space applications: reaction wheel with low power consumption for mini-satellites," IEEE Transactions on Applied Superconductivity, vol. 13, no. 2, pp. 2275- 2278, Jun. 2003.

[37] A. Borisavljevic, H. Polinder, and J. A. Ferreira, "On the Speed Limits of Permanent-Magnet Machines," IEEE Trans. on Industrial Electronics, vol. 57, no. 1, pp. 220-227, Jan. 2010.

[38] S. P. Smith, "The theory of armature windings," Journal of the Institution of Electrical Engineers, vol. 55, no. 261, pp. 18-36, Dec. 1916.

[39] P. L. Alger, E. H. Freiburghouse, and D. D. Chase, "Double Windings for Turbine Alternators," American Institute of Electrical Engineers, Trans. of the, vol. 49, no. 1, pp. 226-244, Jan. 1930.

[40] E. F. Fuchs and L. T. Rosenberg, "Analysis of an Alternator with Two Displaced Stator Windings," IEEE Transactions on Power Apparatus and Systems, vol. 93, no. 6, pp. 1776-1786, Nov. 1974.

[41] A. K. Wallace, R. Spee, and H. K. Lauw, "The potential of brushless doubly-fed machines for adjustable speed drives," Conference Record of 1990 Pulp and Paper Industry Technical Conference, pp. 45-50, Seattle, WA, June 18-22 1990.

[42] M. Touma-Holmberg, and K. Srivastava, "Double winding, high-Voltage cable wound Generator: steady-State and fault analysis," IEEE Trans. on Energy Conversion, Vol. 19, No. 2, pp. 245-50, June 2004.

[43] T. Kataoka and E. H. Watanabe, "Steady-State Characteristics of a Current-Source Inverter/Double-Wound Synchronous Machine System for AC Power Supply," IEEE Trans. on Industry Applications, vol. 16, no. 2, pp. 262-270, Mar. 1980.

[44] T. Kataoka, E. H. Watanabe, and J. Kitano, "Dynamic Control of a Current-Source Inverter/ Double-Wound Synchronous Machine System for AC Power Supply," IEEE Trans. on Industry Applications, vol. 17, no. 3, pp. 314-320, May. 1981.

[45] D. W. Swett and J. G. Blanche, "Flywheel charging module for energy storage used in electromagnetic aircraft launch system," IEEE Trans. on Magnetics, vol. 41, no. 1, pp. 525- 528, Jan. 2005.

[46] M. Leijon, H. Bernhoff and B. Bolund, "System for storage of power", European Patent EP1565337.

[47] Bianchi, N., "Electrical Machine Analysis Using Finite Elements", CRC; 1 edition (June 17, 2005).

[48] F. Caricchi, F. Crescimbini, E. Santini, C. Santucci, "Influence of the radial variation of the Magnet Pitch in slotless Permanent Mag-net Axial flux motors" IEEE Ind. Appl. Society, annual meeting, New Orleans, Louisiana, October 5-9, 1997.

[49] F. Scedil, "Design and development of a high-speed axial-flux permanent-magnet machine," Technische Universiteit Eindhoven, 2001.

[50] Y. Suzuki, A. Koyanagi, M. Kobayashi, and R. Shimada, "Novel applications of the flywheel energy storage system," Energy, vol. 30, no. 11-12, pp. 2128-2143, August 2005.

[51] J. Kobuchi, K. Oobayashi, and R. Shimada, "Windage loss reduction of flywheel/generator system using He and SF_6 gas mixtures," Energy Conversion Engineering Conference, IECEC-97., vol. 3, pp. 1754-1757, Honolulu, HI, USA 1997.

[52] Schaeffler KG, "Rolling bearings", INA FAG catalog, June 2006.

[53] J. Takacs, "Analytical solutions to eddy current and excess losses," COMPEL: The International Journal for Computation and Mathematics in Electrical and Electronic Engineering, vol. 24, no. 4, pp. 1402-1414, 2005.

[54] Y.K.Chin and J.Soulard, "Modelling of Iron Losses in Permanent Magnet Synchronous Motors with Field-weakening Capability for Electric Vehicles," JSAE Paper Number: 20031168, No. 5D-03 Oct, 2002.

[55] S. Eriksson and H. Bernhoff, "Loss evaluation and design optimisation for direct driven permanent magnet synchronous generators for wind power," Applied Energy, vol. 88, no. 1, pp. 265-271, Jan. 2011.

[56] Martin Ranlöf, "Electromagnetic Analysis of Hydroelectric Generators", Digital Comprehensive Summaries of Uppsala Dissertations from the Faculty of Science and Technology, ISSN 1651-6214; 810, 2011.

[57] K. Oberretl, "Eddy Current Losses in Solid Pole Shoes of Synchronous Machines at No-Load and on Load," Power Apparatus and Systems, IEEE Transactions on, vol. 91, no. 1, pp. 152-160, 1972.

[58] O. Drubel and R. L. Stoll, "Comparison between analytical and numerical methods of calculating tooth ripple losses in salient pole synchronous machines," Energy Conversion, IEEE Trans. on, vol. 16, no. 1, pp. 61-67, 2001.

[59] K. Aston and M. V. Kesava Rao, "Pole-face losses due to open slots," Journal of the Institution of Electrical Engineers - Part II: Power Engineering, vol. 88, no. 3, pp. 223-240, Jun. 1941.

[60] P. J. Lawrenson, P. Reece, and M. C. Ralph, "Tooth-ripple losses in solid poles," Proceedings of the Institution of Electrical Engineers, vol. 113, no. 4, pp. 657-662, 1966.

[61] K. Aston and M. V. K. Rao, "Pole-face losses due to open slots on grooved and ungrooved faces," Proceedings of the IEE - Part IV: Institution Monographs, vol. 100, no. 5, pp. 104-113, Oct. 1953.

[62] F. Márquez-Fernández, A. Reinap, and M. Alaküla, "Design, optimization and construction of an electric motor for an Electric Rear Wheel Drive unit application for a hybrid passenger car," XIX International Conference on Electrical Machines (ICEM), Rome, Italy 2010.

[63] S. S. Williamson, A. Emadi, and K. Rajashekara, "Comprehensive Efficiency Modeling of Electric Traction Motor Drives for Hybrid Electric Vehicle Propulsion Applications," Vehicular Technology, IEEE Trans. on, vol. 56, no. 4, 2007.

[64] Alan J. Chapman, Heat Transfer, Prentice Hall; 4 edition, 1984.

[65] C. Micallef, "End winding cooling in electric machines," PhD thesis, Univ. of Nottingham 2006.

[66] D. A. Staton and A. Cavagnino, "Convection Heat Transfer and Flow Calculations Suitable for Analytical Modelling of Electric Machines," in IECON 2006 - 32nd Annual Conference on IEEE Industrial Electronics, pp. 4841-4846, Paris, France 2006.

[67] R. Smyth, "The thermal analysis of fluid flow parallel to rotating surfaces," 32nd Intersociety Energy Conversion Engineering Conf., IECEC-97, vol. 2 pp. 1531-1536, Honolulu, HI , USA 1997,

[68] Z. Kohari and I. Vajda, "Spin-down measurements and loss calculation of multi-layer, multi-pole HTS magnetic bearings," Super-conductor Science and Technology, vol. 18, no. 2, p. S105-S110, Feb. 2005.

[69] J. Soltani, B. Szabados, and J. Hoolboom, "A novel method of measurement of synchronous machine losses using synthetic loading," IEEE Trans. on Instrumentation and Measurement, vol. 51, no. 6, pp. 1228- 1233, Dec. 2002.

[70] Sakai, K., Tabuchi, Y. and Washizu, T. (1993), "Structure and characteristics of new high speed machines with two or three rotor discs", Conference Record of the IEEE Industry Applications Society Annual Meeting, Toronto, Ont., Canada 1993.

[71] W. Fei and P. C. K. Luk, "Design and performance analysis of a high-speed air-cored axial-flux permanent-magnet generator with circular magnets and coils," Electric Machines and Drives Conference, IEMDC'09. IEEE International, pp. 1617-1624, Miami, FL USA 2009,.

[72] W. Z. Fei and P. C. K. Luk, "Design of a 1kW high speed axial flux permanent-magnet machine," 4th IET Conference on Power Electronics, Machines and Drives, PEMD 2008, pp. 230-234, 2008.

[73] P.E. Mason, K. Atallah, and D. Howe, "Hard and soft Magnetic Composites in High Speed Flywheels," ICCM-12 Conference, paper 1057, Paris, July 1999.

[74] Retrieved from: http://www.sura.se/Sura/hp_products.nsf/vOpendocument/97F569BF197A21 FDC1256A3B002FC03C/$FILE/300-35.pdf?OpenElement. , August 2011.

54

Acta Universitatis Upsaliensis

*Digital Comprehensive Summaries of Uppsala Dissertations
from the Faculty of Science and Technology* 845

Editor: The Dean of the Faculty of Science and Technology

A doctoral dissertation from the Faculty of Science and
Technology, Uppsala University, is usually a summary of a
number of papers. A few copies of the complete dissertation
are kept at major Swedish research libraries, while the
summary alone is distributed internationally through
the series Digital Comprehensive Summaries of Uppsala
Dissertations from the Faculty of Science and Technology.